Comprehensive Experimental and Computational Study of η^6-Arene Ruthenium(II) and Osmium(II) Complexes Supported by Sulfur Analogues of β-Diketiminate Ligand

Supporting Information

Crystal O'Connor, Darren C. Lawlor, Conor Robinson, Helge Müller-Bunz
and Andrew D. Phillips*
School of Chemistry, Science South, University College Dublin, Belfield, Dublin 4, Ireland

Table of Contents

Instrumentation Details

NMR spectra were recorded using a Varian VNMRS 300 or 400 instrument. Where necessary, ^{1}H (COSY, NOE, NOESY), ^{19}F, ^{11}B, $^{31}P\{^{1}H\}$, $^{13}C\{^{1}H\}$ one- and two-dimensional (HMBC and HSQC) spectra were used to assign molecular connectivity and conformation in solution. Deuterated dichloromethane was distilled over CaH_2 and stored over 4 Å molecular sieves. Chemical shifts for ^{1}H and ^{13}C spectra were referenced to the relevant solvent peaks. ^{19}F NMR spectra were referenced to the relevant residual solvent peak and CCl_3F. Elemental microanalyses were obtained using an Exeter Analytical EA-1110 elemental analyzer. Mass spectra were recorded using either solution or nano-electrospray ionization (ESI) technique on a Waters alliance HT Micromass Quattro LCT ($MeOH/H_2O$, 60 to 40 ratio) TOF instrument with a cone voltage of 35 V and a capillary voltage of 2800 V (+) and 2500 V (-). UV-visible spectra were collected using an Agilent Technologies Carey 60 instrument equipped with a Xenon light source. All samples were measured under an inert atmosphere of N_2 in quartz cuvettes sealed with a Teflon stopper. Solid-state infrared data was collected using a Bruker precision spectrometer equipped with an attenuated total reflectance diamond crystal. Crystal data were collected using a Rigaku Oxford Diffraction (former Agilent Technologies, former Oxford Diffraction) SuperNova diffractometer fitted with an Atlas detector, or an Oxford Diffraction Kuma diffractometer (**13**) or in the case of **2c**, a Bruker-Nonus KappaCCD with Apex II CCD. The crystals were kept under a 140 or 100 K gaseous flow of N_2 during the collection procedure. All Complexes were measured with Cu-Kα (1.54184 Å), except for **2c**, **5c**, **7c** and **13** which were measured using Mo-Kα (0.71073 Å). Data collection was performed using CrysAlis Pro[1] (Oxford diffractometers) or Collect/EvalCCD[2,3] and processed with SAINT.[4] A doubly redundant dataset was collected assuming all Friedel pairs are inequivalent. Cell parameter refinement and space group determination was done through CrysAlis Pro or with a combination of Dirax and XPREP.[5,6] An analytical absorption correction based on the shape of the crystal was performed, using CrysAlis Pro or SADABS.[7] The structures were solved by direct methods using SHELXS-97 or SHELXS-2014[8] and refined by full matrix least-squares on F^2 for all data using SHELXL-97 or SHELXS-2014.[8] Hydrogen atoms were added at calculated positions and refined using a riding model. The isotropic temperature factors for the hydrogen atoms were fixed to 1.2 times (1.5 times for methyl groups) the equivalent isotropic displacement parameters of the carbon atom to which the hydrogen is attached. Anisotropic thermal displacement parameters were used for all non-hydrogen atoms. Some groups, especially the η^6-arene in complex **8** and CF_3 groups of the BArF counter-ion were disordered. In these cases, the affected atoms were split, and the site occupancy of the disordered atom group was allowed to refine. In cases where the solvate demonstrated significant disorder, its contribution to the overall structure factors was removed using the SQUEEZE algorithm developed by Spek *et al.*[9] All ORTEP drawing were performed using the ORTEP-3 program developed by Farrugia.[10]

General *in-situ* synthesis of Li-β-thioketoiminate complexes

The selected β-thioketoiminate (1 equiv. 4 mmol) was dissolved in dry *n*-pentane (10 mL) and the flask cooled to below 0 °C using a salt-ice bath. *n*-Butyllithium (1.6M in hexanes, 1.2 equiv., 4.8 mmol) was added dropwise to instantly afford a dark red-brown solution.[48] After stirring for 3 hours, under N_2, the solvent was removed to give the product as a red-brown powder. The resulting mixture was used directly in the subsequent metal coordination reactions without analysis.

Characterization of β-thioketoiminate ligands 3a-d and β-selenoketoiminates 4b-c.

***N*-phenyl-β-thioketoiminate (3a):** Red crystalline solid with a yield of 17%. Due to instability of the product, a satisfactory elemental analysis could not be obtained. MS-TOF-ES (positive mode, m/z): 190.0596 (100%, calculated: 191.2937). ^{1}H NMR (25 °C, 400 MHz, $CDCl_3$), δ(ppm): 2.12 (s, 3H, α-NCC*H*$_3$), 2.60 (s, 3H, α-SCC*H*$_3$), 6.26 (s, 1H, β-C*H*), 7.20-7.21 (m, 2H, Ar *m*-C*H*), 7.29–7.32 (m, 1H, Ar *p*-C*H*), 7.39–7.43 (m, 2H, Ar *o*-C*H*), 15.56 (s, 1H, N*H*). ^{13}C{^{1}H} NMR (25°C, 100 MHz, $CDCl_3$), δ(ppm): 21.3 (NCCH_3), 39.0 (α-SCCH_3), 133.8 (β-*C*H), 125.3 (Ar *m*-*C*H), 127.0 (Ar *p*-*C*H), 129.3 (Ar *o*-*C*H), 137.2 (Ar *i*-*C*), 163.5 (α-N*C*CH_3), 207.6 (*C*=*S*). Both ^{1}H and ^{13}C{^{1}H} NMR spectra are shown on page S10.

***N*-2,6-Dimethylphenyl-β-thioketoiminate (3b)**: Red crystalline solid with a yield of 69%. Elemental Analysis for $C_{13}H_{17}NS$: Found (Calculated) C 70.87 (71.18), H 7.67 (7.81), N: 6.60 (6.39), S 14.63 (14.62). MS-TOF-ES (positive mode), (m/z): 220.1124 (100%, calculated. 219.1966). ^{1}H NMR (25 °C, 400 MHz, $CDCl_3$), δ(ppm): 1.81 (s, 3H, α-NCC*H*$_3$), 2.22 (s, 6H, Ar *o*-CC*H*$_3$), 2.63 (s, 3H, α-SCC*H*$_3$), 6.32 (s, 1H, β-C*H*), 7.11–7.16 (m, 3H, Ar C*H*), 15.21 (s, 1H, N*H*). ^{13}C{^{1}H} NMR (25 °C, 100 MHz, $CDCl_3$), δ(ppm): 18.3 (Ar *o*-C*C*H_3), 20.5 (α-NC*C*H_3), 38.8 (SC*C*H_3), 112.9 (β-*C*H), 127.9 (Ar *p*-*C*H), 128.4 (Ar *m*-*C*H), 134.8 (Ar *o*-*C*CH_3), 135.6 (Ar *i*-*C*), 166.9 (α-N*C*CH_3), 206.9 (*C*=*S*).

***N*-2,6-Diisopropylphenyl-β-thioketoiminate (3c)**: Red crystalline solid with a yield of 89%. Elemental Analysis for $C_{17}H_{25}NS$•0.05CH_2Cl_2: Found (Calculated) C 73.38 (73.22), H 9.07 (9.05), N 5.12 (5.01), S 11.23 (11.46). MS-TOF-ES (positive mode), (m/z): 276.1779 (100%, calculated. 276.1786). ^{1}H NMR (25 °C, 400 MHz, $CDCl_3$), δ(ppm): 1.22 (d, $^3J_{HH}$ = 6.8 Hz, 6H, Ar *o*-CH(C*H*$_3$)), 1.25 (d, $^3J_{HH}$ = 6.9 Hz, 6H, Ar *o*-CH(C*H*$_3$)), 1.84 (s, 1H, α-NCC*H*$_3$), 2.67 (s, 1H, α-SCC*H*$_3$), 2.97 (sept, $^3J_{HH}$ = 6.8 Hz, 2H, Ar *o*-C*H*(CH_3)), 6.35 (s, 1H, β-C*H*), 7.24–7.26 (m, 2H, Ar m-C*H*), 7.35–7.39 (m, 1H, Ar *p*-C*H*), 15.30 (s, 1H, N*H*). ^{13}C{^{1}H} NMR (25 °C, 100 MHz, $CDCl_3$) δ(ppm): 20.9 (Ar *o*-*C*H(CH_3), 22.5 (Ar *o*-CH(*C*H_3), 25.0 (α-NC*C*H_3), 28.7 (Ar *o*-*C*H(CH_3)), 38.8 (α-SC*C*H_3), 112.7 (β-*C*H), 123.6 (Ar *p*-*C*H), 128.9 (Ar *m*-*C*H), 132.4 (Ar *o*-*C*H(C*H*$_3$)), 145.1 (Ar *i*-*C*), 166.3 (α-N*C*CH_3), 206.9 (*C*=*S*).

***N*-2,6-Dimethylphenyl-α-trifluoromethyl-β-thioketoiminate (3d)**: Red-orange crystalline plates with a yield of 79%. Elemental Analysis for $C_{13}H_{14}F_3NS$•0.05CH_2Cl_2: Found (Calculated) C 56.51 (56.47), H 5.02 (5.12), N 4.81 (5.05), S 11.05 (11.55), F: 21.04 (20.53). MS TOF ES (positive mode, m/z): 274.0885 (100%, calculated: 274.0877). ^{1}H NMR (25 °C, 400 MHz, $CDCl_3$), δ(ppm): 1.97 (s, 3H, β-NCC*H*$_3$), 2.22 (s, 6H, Ar *o*-C*H*$_3$), 6.84 (s, 1H, β-C*H*), 7.16–7.18 (m, 2H, Ar *m*-C*H*), 7.22–7.24 (m, 1H, Ar *p*-C*H*), 15.46 (s, 1H, N*H*). ^{13}C{^{1}H} NMR (25 °C, 100 MHz, $CDCl_3$) δ(ppm): 18.4 (Ar *o*-C*C*H_3), 21.0 (α-NC*C*H_3), 111.6 (β-*C*H), 121.9 (Ar *p*-*C*H), 128.9 (Ar *m*-*C*H), 134.2 (Ar *o*-*C*CH_3), 134.6

(Ar *i-C*), 170.1(α-N*C*CH$_3$), 184.0 (*C=S*). (q, $^1J_{CF}$ = 132 Hz, α-SC*C*F$_3$). ^{19}F NMR (25 °C, 376 MHz, CDCl$_3$) δ (ppm): -68.00 (C*F*$_3$).

***N*-2,6-Dimethylphenyl-β-selenoketoiminate (4b):** A red oil with a yield of 60%. Due to instability of the product, a satisfactory elemental analysis could not be obtained. ^{1}H NMR (25 °C, 400 MHz, CDCl$_3$), δ(ppm): 1.70 (s, 3H, α-NCC*H*$_3$), 2.24 (s, 6H, Ar *o*-CC*H*$_3$), 2.67 (s, 3H, α-SeCC*H*$_3$), 6.68 (s, 1H, β-C*H*), 7.15–7.16 (m, 3H, Ar C*H*), 15.60 (s, 1H, N*H*). ^{13}C{^{1}H} NMR (25 °C, 100 MHz, CDCl$_3$), δ(ppm): 18.5 (Ar *o*-C*C*H$_3$), 21.4 (α-NC*C*H$_3$), 42.9 (α-SeC*C*H$_3$), 118.5 (β-C*H*), 128.2 (Ar *p-C*H), 128.6 (Ar *m-C*H), 134.6 (Ar *o-C*CH$_3$), 135.3 (Ar *i-C*), 167.0 (α-N*C*CH$_3$), 204.6 (*C=Se*). The ^{1}H NMR spectrum is shown on page S11.

***N*-2,6-Diisopropylphenyl-β-selenoketoiminate (4c):** Obtained as a red oil with a yield of 51%. Due to instability of the product, a satisfactory elemental analysis could not be obtained. ^{1}H NMR (25 °C, 400 MHz, CDCl$_3$), δ(ppm): 1.19-1.24 (d, $^3J_{HH}$ = 6.8 Hz, 6H, Ar *o*-CH(C*H*$_3$)), 1.27–1.28 (d, $^3J_{HH}$ = 6.8 Hz, 6H, Ar *o*-CH(C*H*$_3$)), 1.69 (s, 1H, α-NCC*H*$_3$), 2.68 (s, 1H, α-SCC*H*$_3$), 2.90–2.97 (m, 2H, Ar *o*-C*H*(CH$_3$)), 6.67 (s, 1H, β-C*H*), 7.03–7.05 (m, 2H, Ar *m*-C*H*), 7.22–7.26 (m, 1H, Ar *p*-C*H*), 15.64 (s, 1H, N*H*). ^{13}C{^{1}H} NMR (25 °C, 100 MHz, CDCl$_3$) δ (ppm): 20.9 (Ar *o*-CH(*C*H$_3$), 22.5 (Ar *o*-CH(*C*H$_3$), 25.0(α-NC*C*H$_3$), 28.7 (Ar *o-C*H(CH$_3$)), 38.8 (α-SeC*C*H$_3$), 112.7 (β-C*H*), 123.6 (Ar *p-C*H), 128.9 (Ar *m-C*H), 132.4 (Ar *o-C*), 145.1 (Ar *i-C*), 166.3(α-N*C*CH$_3$), 206.9 (*C=Se*).

Characterization of chloro arene-Ru(II) or -Os(II)-β-thioketoiminate complexes 5a-c and 6.

Chloro-(η^6-benzene)-ruthenium(II)-*N*-phenyl-β-thioketoiminate (5a): Dark brown powder with a yield of 44%. Decomposition prevented accurate elemental analysis. MS TOF-ES (positive mode, m/z): 370.0244 (100%, calculated [M$^+$-Cl]: 370.0203). ^{1}H NMR (25 °C, 400 MHz, CD$_2$Cl$_2$), δ(ppm): 1.63 (s, 3H, α-NCC*H*$_3$), 2.19 (s, 3H, α-SCC*H*$_3$), 4.91 (s, 6H, C$_6$*H*$_6$), 5.75 (s, 1H, β-C*H*), 7.14–7.17 (m, 2H, Ar *o*-C*H*), 7.36–7.38 (s, 3H, Ar *m,p*-C*H*). ^{13}C{^{1}H} NMR (25 °C, 100 MHz, CD$_2$Cl$_2$) δ(ppm): 26.4 (α-NC*C*H$_3$), 29.5 (α-SC*C*H$_3$), 87.0 (*C*$_6$H$_6$), 116.9 (β-*C*H), 125.5 (Ar *p-C*H), 128.2 (Ar *m-C*H), 128.7 (Ar *o-C*H), 159.7 (Ar *i-C*), 166.1 (α-N*C*CH$_3$), 166.7 (α-S*C*CH$_3$).

Chloro-(η^6-benzene)-ruthenium(II)-*N*-2,6-dimethylphenyl-β-thioketoiminate (5b): Dark brown powder with a yield of 81%. Decomposition prevented accurate elemental analysis. MS TOF-ES (positive mode, m/z): 398.0514 (100%, calculated [M$^+$-Cl]: 398.0516). ^{1}H NMR (25 °C, 400 MHz, CD$_2$Cl$_2$), δ(ppm): 1.54 (s, 3H, α-NCC*H*$_3$), 2.24 (s, 3H, α-SCC*H*$_3$), 2.34 (s, 6H, Ar *o*-CC*H*$_3$), 4.93 (s, 6H, C$_6$*H*$_6$), 5.88 (s, 1H, β-C*H*), 7.05–7.09 (m, 1H, Ar *p*-C*H*), 7.18–7.20 (m, 2H, Ar *m*-C*H*). ^{13}C{^{1}H} NMR (25 °C, 100 MHz, CD$_2$Cl$_2$) δ(ppm): 18.2 (Ar *o*-C*C*H$_3$), 23.5 (α-NC*C*H$_3$), 29.4 (α-SC*C*H$_3$), 86.8 (*C*$_6$H$_6$), 120.0 (β-*C*H), 125.8 (Ar *p-C*H), 128.6 (Ar *m-C*H), 130.1 (Ar *o-C*CH$_3$), 156.6 (Ar *i-C*N), 166.3 (α-N*C*CH$_3$), 166.5 (α-S*C*CH$_3$).

Chloro-(η^6-benzene)-ruthenium(II)-β-N-2,6-diisopropylphenyl-thioketoiminate (5c): Red-brown powder with a yield of 89%. Elemental Analysis for $C_{23}H_{30}Ru_1N_1S_1Cl_1$•0.07$CH_2Cl_2$: Found (Calculated) C 51.77(51.89), H 5.64 (5.77), N 2.55 (2.55). MS-TOF-ES (positive mode, m/z): 454.1139 (100%, calculated [M$^+$-Cl]: 454.1142). ^{1}H NMR (25 °C, 400 MHz, CD$_2$Cl$_2$), δ(ppm): 1.06 (d, $^3J_{HH}$ = 6.7 Hz, 6H, Ar *o*-CH(C*H*$_3$)), 1.39 (d, $^3J_{HH}$ = 6.7 Hz, 6H, Ar *o*-C*H*(CH$_3$)), 1.69 (s, 1H, α-

NCC*H*$_3$), 2.24 (s, 1H, α-SCC*H*$_3$), 3.53 (m, 2H, Ar *o*-C*H*(CH$_3$)), 4.99 (s, 6H, C$_6$*H*$_6$), 5.85 (s, 1H, β-C*H*), 7.24–7.26 (m, 3H, Ar *m,p*-C*H*). ^{13}C NMR (25 °C, 100 MHz, CD$_2$Cl$_2$) δ(ppm): 24.2 (Ar *o*-CH(*C*H$_3$), 25.4 (NC*C*H$_3$), 26.4 (Ar *o*-CH(*C*H$_3$), 28.0 (Ar *o*-CH(*C*H$_3$), 29.9 (α-SC*C*H$_3$), 87.3 (*C*$_6$H$_6$), 120.4 (β-*C*H), 127.3 (Ar-C), 154.1 (Ar-C), 165.3 (α-S*C*CH$_3$). Not all signals were observed. UV-Visible (25°C, CH$_2$Cl$_2$), λ_{max} (nm) [ε (L mol^{-1} cm^{-1})]: 488 [1.07 × 10^4], 370 [2.62 × 10^4].

Chloro-(η^6-benzene)-osmium(II)-β-N-2,6-diisopropylphenyl-thioketoiminate (6): Red-brown powder with a yield of 89%. Elemental Analysis for C$_{23}$H$_{30}$Cl$_1$N$_1$Os$_1$S$_1$•0.65CH$_2$Cl$_2$ Found (Calculated) C: 44.92 (44.85), H: 5.00 (4.98); N: 2.01 (2.21). MS-TOF-ES (positive mode), (m/z): 544.1722 (100%, calculated [M$^+$-Cl]: 544.1714). ^{1}H NMR (25 °C, 400 MHz, CDCl$_3$), δ(ppm): 1.08 (d, ^{3}J$_{HH}$ = 6.8 Hz, 6H, Ar *o*-CH(C*H*$_3$)), 1.34 (d, ^{3}J$_{HH}$ = 6.8 Hz, 6H, Ar *o*-CH(C*H*$_3$)), 1.59 (sept, ^{3}J$_{HH}$ = 6.8 Hz, 2H, Ar *o*-C*H*(CH$_3$)), 1.74 (s, 1H, α-NCC*H*$_3$), 2.35 (s, 1H, α-SCC*H*$_3$), 5.16 (s, 6H, C$_6$*H*$_6$), 6.04 (s, 1H, β-C*H*), 7.18–7.28 (m, 3H, Ar *m,p*-C*H*). ^{13}C{^{1}H} NMR (25 °C, 100 MHz, CDCl$_3$) δ(ppm): 24.4 (Ar *o*-CH(*C*H$_3$)), 25.3 (α-NC*C*H$_3$), 26.7 (Ar *o*-CH(*C*H$_3$)), 27.6(Ar *o*-*C*H(CH$_3$)), 30.1 (α-SC*C*H$_3$), 30.4, 78.2 (*C*$_6$H$_6$), 120.9 (β-*C*H), 124.2 (Ar-C), 127.3 (Ar-C), 141.4 (Ar-C), 167.4 α-S*C*CH$_3$). Not all signals were observed. UV-Visible (25°C, CH$_2$Cl$_2$), λ_{max} (nm) [ε (L mol^{-1} cm^{-1})]: 484 [9.07 × 10^3], 324 [2.64 × 10^4].

Characterization of salts containing the cationic (η^6-C$_6$H$_6$) Ru(II) or Os(II)-β-thioketoiminate complexes 7b-c and 8.

(η^6-benzene)-ruthenium(II)-β-N-2,6-dimethylphenyl-thioketoiminate triflate (7b): Using method B, a dark brown powder was obtained with 40 % yield. Elemental Analysis for C$_{20}$H$_{22}$F$_3$NO$_3$RuS$_2$. Found (Calculated): C 43.95 (47.09), H 4.08 (4.52); N: 2.56 (2.75). MS TOF-ES (positive mode), m/z): 398.0505 (100%, calculated. 398.0516). ^{1}H NMR (25 °C, 400 MHz, CD$_2$Cl$_2$), δ(ppm): 1.64 (s, 6H, Ar *o*-CC*H*$_3$), 2.30 (s, 3H, α-NCC*H*$_3$), 2.36 (s, 3H, α-SCC*H*$_3$), 5.04 (s, 6H, C$_6$*H*$_6$), 6.06 (s, 1H, β-C*H*), 7.09–7.13 (m, 1H, Ar *p*-C*H*), 7.21-7.23 (m, 2H, Ar *m*-C*H*). ^{13}C{^{1}H} NMR (25 °C, 100.6 MHz, CD$_2$Cl$_2$) δ(ppm): 18.9 (Ar *o*-C*C*H$_3$), 24.3 (α-NC*C*H$_3$), 29.9 (α-SC*C*H$_3$), 87.1 (*C*$_6$H$_6$), 120.5 (β-*C*H), 126.6 (Ar *p*-*C*H), 128.8 (Ar *o*-*C*CH$_3$), 129.1 (Ar *m*-*C*H), 157.6 (Ar *i*-*C*), 166.3 (α-N*C*CH$_3$), 167.9 (α-S*C*CH$_3$). ^{19}F NMR (25 °C, 376 MHz, CD$_2$Cl$_2$) δ(ppm): -77.66 (SO$_3$C*F*$_3$).

(η^6-benzene)-ruthenium(II)-*N*-2,6-dimethylphenyl-β-thioketoiminate hexafluorophosphate (7b): Employing method A, a dark brown powder was obtained with a yield of 33 %. MS TOF-ES (positive mode, m/z): 397.7708 (100%, calculated: 397.5207). ^{1}H NMR (25 °C, 400 MHz, CD$_2$Cl$_2$), δ(ppm): 2.01 (s, 6H, Ar *o*-CC*H*$_3$), 2.28 (s, 3H, α-NC*C*H$_3$), 3.15 (s, 3H, α-SCC*H*$_3$), 5.80 (s, 6H, C$_6$*H*$_6$), 6.22 (s, 1H, β-C*H*), 7.35–7.37 (m, 1H, Ar *p*-C*H*), 7.41-7.43 (m, 2H, Ar *o*-C*H*). ^{13}C{^{1}H} NMR (25 °C, 100 MHz, CD$_2$Cl$_2$) δ(ppm): 18.5 (Ar *o*-C*C*H$_3$), 25.4 (α-NC*C*H$_3$), 29.5 (α-SC*C*H$_3$), 84.7 (*C*$_6$H$_6$), 119.4 (β-*C*H), 127.9 (Ar *p*-*C*H), 129.1 (Ar *o*-*C*CH$_3$), 129.2 (Ar *m*-*C*H), 159.3 (Ar *i*-*C*), 168.2 (α-N*C*CH$_3$), 173.9 (*C*=*S*). ^{19}F NMR (25 °C, 376 MHz, CD$_2$Cl$_2$) δ ppm: -72.40 (d, ^{1}J$_{PF}$ = 711.6 Hz, P*F*$_6$). ^{31}P{^{1}H} NMR (25 °C, 161.89 MHz, CD$_2$Cl$_2$) δ(ppm): -144.37 (sept, ^{1}J$_{PF}$ = 710.1 Hz, *P*F$_6$). Both ^{1}H and ^{13}C NMR spectra are shown on page S12.

(η^6-benzene)-ruthenium(II)-*N*-2,6-diisopropylphenyl-β-thioketoiminate triflate (7c): Using method A, a red-brown powder was obtained with a 40% yield. Elemental Analysis for C$_{24}$H$_{30}$F$_3$NO$_3$RuS$_2$•0.2CH$_2$Cl$_2$. Found (Calculated) C 46.67 (46.91), H 5.21 (4.94), N 2.71 (2.26). MS

TOF-ES (positive mode, m/z): 454.1130 (100%, calculated: 454.1142). ^{1}H NMR (25 °C, 400 MHz, CD_2Cl_2), δ ppm: 1.06 (d, $^3J_{HH}$ = 6.8 Hz, 6H, Ar *o*-CH(C*H*$_3$)), 1.39 (d, $^3J_{HH}$ = 6.8 Hz, 6H, Ar *o*-CH(C*H*$_3$)), 1.70 (s, 1H, α-NCC*H*$_3$), 2.27 (s, 1H, α-SCC*H*$_3$), 3.50 (m, 2H, Ar *o*-CH(CH$_3$)), 5.01 (s, 6H, C$_6$*H*$_6$), 5.89 (s, 1H, β-C*H*), 7.27-7.31 (m, 3H, Ar *m,p*-C*H*). ^{13}C{^{1}H} NMR (25 °C, 100 MHz, CD_2Cl_2) δ ppm: 24.3 (Ar *o*-CH(*C*H$_3$)), 25.4 (α-NC*C*H$_3$), 26.5 (Ar *o*-CH(*C*H$_3$)), 28.1 (Ar *o*-*C*H(CH$_3$)), 29.9 (α-SC*C*H$_3$), 87.3 (*C*$_6$H$_6$), 120.5 (β-*C*H), 124.8 (Ar-C), 127.4 (Ar-C), 141.1 (Ar-C), 154.4 (Ar-C), 165.8 (α-N*C*CH$_3$), 167.6 (C=S). ^{19}F NMR (25 °C, 376 MHz, CD_2Cl_2) δ(ppm): -78.86 (SO$_3$C*F*$_3$).

(η^6-benzene)-ruthenium(II)-*N*-2,6-diisopropylphenyl-β-thioketoiminate tetrakis-3,5-trifluoro-methylphenyl-borate (7c): Employing method A, a dark red powder was obtained with a 77 % yield. Elemental Analysis for $C_{55}H_{42}B_1F_{24}N_1S_1Ru$•0.3$CH_2Cl_2$. Found (Calculated) C 49.51 (49.48), H 3.11 (3.20), N 0.98 (1.04). MS TOF-ES positive mode: (m/z) 454.1155 (100%, calculated: 454.1142). ^{1}H NMR (25 °C, 400 MHz, CD_2Cl_2), δ(ppm): 1.05 (d, $^3J_{HH}$ = 6.8 Hz, 6H, Ar *o*-CH(C*H*$_3$)), 1.30 (d, $^3J_{HH}$ = 6.8 Hz, 6H, Ar *o*-*C*H(*CH*$_3$)), 2.41 (s, 1H, α-NCC*H*$_3$), 2.42–2.48 (m, $^3J_{HH}$ = 6.8 Hz, 2H, Ar *o*-C*H*(CH$_3$)), 3.11 (s, 1H, α-SCC*H*$_3$), 5.79 (s, 6H, C$_6$*H*$_6$), 7.39 (s, 1H, β-C*H*), 7.47–7.54 (m, 3H, Ar *m,p*-C*H*), 7.56 (br s, 4H, *p*-C*H* (BAr^F$_4$)), 7.73 (br s, 8H, *o*-C*H* (BAr^F$_4$)). ^{13}C{^{1}H} NMR (25 °C, 100 MHz, CD_2Cl_2) δ(ppm): 24.2 (Ar *o*-CH(*C*H$_3$)), 25.2 (α-NC*C*H$_3$), 28.2 (Ar *o*-CH(*C*H$_3$)), 29.3 (Ar *o*-*C*H(CH$_3$)), 29.8 (α-SC*C*H$_3$), 85.0 (*C*$_6$H$_6$), 118.0 (β-*C*H), 119.4 (Ar-C), 123.8 (Ar-C), 125.2 (Ar-C), 126.5 (Ar-C), 129.6 (Ar-C), 135.4 (Ar-C), 140.3 (Ar-C), 157.1, 162.1 (q, $^1J_{BC}$ = 50 Hz, Ar *i*-*C*B),170.1 (α-N*C*CH$_3$), 173.5 (C=S). ^{11}B NMR (25 °C, 128 MHz, CD_2Cl_2) δ(ppm): -6.63 (*B*Ar^F$_4$). ^{19}F NMR (25 °C, 376 MHz, CD_2Cl_2) δ(ppm): -62.83 (BAr^F$_4$). UV-Visible (25°C, CH_2Cl_2), λ_{max} (nm) [ε (L mol^{-1} cm^{-1})]: 530 [1.88 × 10^3], 423 [3.08 × 10^3], 324 [1.31 × 10^4], 279 [2.05 × 10^4], 264 [2.83 × 10^4].

(η^6-benzene)-osmium(II)-*N*-2,6-diisopropylphenyl-β-thioketoiminate tetrakis-3,5-trifluoro-methylphenyl-borate (8): Employing method A, using 0.100 g of the Os precursor, a brown powder was obtained (0.180 g) with a yield of 68%. Elemental Analysis: Calculated for $C_{55}H_{42}B_1F_{24}$N1OsS•0.75CH_2Cl_2 Found (Calculated): C 45.82 (45.56), H: 2.87 (2.98), N: 0.65 (0.95). MS TOF-ES positive mode: (m/z) 544.1724 (100%, calculated M$^+$: 544.1714). ^{1}H NMR (25 °C, 400 MHz, CD_2Cl_2), δ(ppm): 1.08 (d, $^3J_{HH}$ = 6.6 Hz, 6H, Ar *o*-CH(C*H*$_3$)), 1.27 (d, $^3J_{HH}$ = 6.6 Hz, 6H, Ar *o*-CH(C*H*$_3$)), 2.49 (m, $^3J_{HH}$ = 6.6 Hz, 2H, Ar *o*-C*H*(CH$_3$)), 2.52 (s, 1H, α-NCC*H*$_3$), 3.18 (s, 1H, α-SCC*H*$_3$), 6.38 (s, 6H, C$_6$*H*$_6$), 7.37–7.51 (m, 3H, Ar *m,p*-C*H*), 7.56 (br s, 4H, *p*-C*H* (BAr^F$_4$)), 7.72 (br s, 8H, *o*-C*H* (BAr^F$_4$)). 7.83 (s, 1H, β-C*H*). ^{13}C{^{1}H} NMR (25 °C, 100 MHz, CD_2Cl_2) δ(ppm): 24.4 (Ar *o*-CH(*C*H$_3$)), 25.3 (α-NC*C*H$_3$), 28.9 (Ar *o*-CH(*C*H$_3$)), 29.3 (Ar *o*-*C*H(CH$_3$)), 30.07 (α-SC*C*H$_3$), 78.9 (*C*$_6$H$_6$), 118.1 (β-*C*H), 122.3 (Ar-C), 123.8 (Ar-C), 124.8 (Ar-C), 126.5 (Ar-C), 129.2 (Ar-C), 129.6 (Ar-C), 130.0 (Ar-C), 135.4 (Ar-C), 140.2 (Ar-C), 162.3 (q, $^1J_{BC}$ = 50 Hz, Ar *i*-*C* (BAr^F$_4$)), 170.3 (N*C*CH$_3$), 176.1 (C=S). ^{11}B NMR (25 °C, 128MHz, CD_2Cl_2) δ ppm: -6.58 (*B*Ar^F$_4$). ^{19}F NMR (25 °C, 376 MHz, CD_2Cl_2) δ(ppm): -62.83 (BAr^F$_4$). UV-Visible (25°C, CH_2Cl_2), λ_{max} (nm) [ε (L mol^{-1} cm^{-1})]: 507 [1.04 × 10^3], 432 [1.48 × 10^3], 311 [1.14 × 10^4], 279 [1.37 × 10^4], 270 [1.39 × 10^4].

Specific procedures for the synthesis and characterization of complexes 2c, 2d, 10, 11, 12 and 13.

(η^6-benzene)-ruthenium(II)-2,6-diisopropylphenyl-β-diketiminate triflate (2c): This complex was prepared using a method which was modified to that previously reported by Phillips *et al*. for complex **2a**, (η^6-C$_6$H$_6$)-Ru-[(2,6-((CH$_3$)$_2$)C$_6$H$_3$)$_2$NC(CH$_3$))$_2$CH]SO$_3$CF$_3$.[11] To a dried 50 mL round bottom flask, 0.125 g (0.500 mmol) of ((η^6-C$_6$H$_6$)RuCl$_2$)$_2$ was combined with 0.090 g (0.523 mmol) of [Na]O$_3$SCF$_3$,

then 10 mL of CH_2Cl_2 was added affording an orange suspension. Subsequently, a freshly prepared solution consisting of 0.172 g (0.508 mmol) of Li-[(2,6-$(CH(CH_3)_2)_2C_6H_3)_2NC(CH_3))_2CH$[12] was dissolved with 5 mL of CH_2Cl_2. This solution was added dropwise to the flask containing the Ru-based precursor over a period of 45 minutes. The flask was capped, and the reaction mixture stirred overnight. The resulting dark-brown solution was filtered through celite frit combination. The contents of the frit were washed with CH_2Cl_2 until the resulting filtrate was colorless. Employing reduced pressure, the volume of the solution was concentrated to approximately 1 mL. While stirring rapidly, 25 mL of diethyl ether was rapidly added, causing the formation of a dark-brown precipitate, which was collected on a frit and washed 2 times with 5 mL portions of Et_2O and then 3 times with 5 mL portions of *n*-pentane. The solid was dried for 12 hours under reduced pressure. A total of 0.165 g (0.255 mmol) was obtained resulting in a 50.9% yield. Crystals suitable for single X-ray diffraction were obtained by slow diffusion of *n*-pentane into a saturated chloroform solution. Elemental analysis for $C_{36}H_{47}F_3N_2O_3RuS$•$0.4CH_2Cl_2$: Found (Calculated): C: 56.26 (56.06), H: 5.89 (6.18), N: 3.43 (3.59). ESI-MS (25°C, CH_2Cl_2), positive mode: (m/z) 597.267 (100%). Negative mode: (m/z) 149.202 (100%). ^{1}H NMR (25 °C, 400 MHz, CD_2Cl_2) δ(ppm) 1.149 (d, $^3J_{HH}$ = 6.85 Hz, 12H, Ar $(CH_3)_2{}^A$CH), 1.437 (d, $^3J_{HH}$ = 6.85 Hz, 12H, Ar $(CH_3)_2{}^B$CH), 2.329 (s, 6H, α-CH_3), 2.746 (sept, $^3J_{HH}$ = 6.85 Hz, 4H, Ar $(CH_3)_2CH$), 5.252 (s, 6H, C_6H_6 *CH*) 6.617 (s, 1H, β-*CH*), 7.474 (m, $^3J_{HH}$ = 1.95 Hz, 4H, Ar *m*-CH), 7.529 (m, $^3J_{HH}$ = 1.95 Hz, 2H, Ar *p*-CH). Note: A denotes the CH_3 group pointing away from the η^6-arene. B denotes the CH_3 group pointing towards the η^6-arene ring. Determined by NOE radiation of the η^6-arene protons at δ(^{1}H) = 5.3 ppm. $^{13}C\{^1H\}$ NMR (25 °C, 100 MHz, CD_2Cl_2) δ(ppm) 24.38 (s, α-CH_3), 25.07 (s, $CH(CH_3)_2$), 25.46 (s, $CH(CH_3)_2$), 29.23 (s, $CH(CH_3)_2$), 83.82 (s, C_6H_6 *C*H), 104.56 (s, β-*C*H), 125.08 (s, Ar *m*-*C*H), 128.23 (s, Ar *p*-*C*H), 140.57 (s, Ar *o*-*C*), 155.90 (s, Ar *i*-*C*), 164.86 (s, α-N*C*CH_3). ^{19}F NMR (25 ºC, 376 MHz, CD_2Cl_2) δ(ppm): -79.1 ($^1J_{FC}$ = 321 Hz, SO_3CF_3). IR (FT-ATR-diamond, 25 °C, solid), υ(cm^{-1}): 3054.85(w), 2963.38(w), 2928.27(w), 2869.19(w), 1556.82(w), 1464.13(w), 1434.22(w), 1387.06(w), 1364.86(w), 1346.87(w), 1314.94(w), 1292.82(w), 1264.13(s), 1221.77(m), 1150.48(s), 1102.10(w), 1055.29(w), 1030.70(s), 986.49(w), 933.33(w), 866.98(w), 835.68(w), 798.50(m), 761.35(m), 753.58(w), 721.51(w). UV-Visible (25°C, CH_2Cl_2), λ_{max} (nm) [ε (L mol^{-1} cm^{-1})]: 437 [7.89×10^3], 290 [1.90×10^4].

(η^6-benzene)-osmium(II)-2,6-diisopropylphenyl-β-diketiminate triflate (2d): A 100 mL Schlenk flask was charged with 0.300 g (0.71 mmol) of $(2,6\text{-}(CH(CH_3)_2)C_6H_3NCCH_3)_2CH_2$[12] and dissolved in 25 mL *n*-pentane. The reaction flask was cooled to 4°C using an ice water bath. A 1.6 M solution of *n*-BuLi (1.2 equiv. 0.53 mL, 0.85 mmol) was added dropwise to the solution and stirred under N_2 for 3 hours. The solvent was removed under reduced pressure resulting in a colorless solid. A separate Schlenk flask was charged with 0.179 mg (0.35 mmol) of $((\eta^6\text{-}C_6H_6)OsCl_2)_2$ dimer and $[Na]O_3SCF_3$ (1.2 equiv. 0.85 mmol). After the addition of 10 mL of CH_2Cl_2, a suspension was obtained. Slowly, the contents of the first Schlenk flask were added to second flask using a syringe. After overnight stirring, the resulting brown colored solution was filtered through celite and the solvent reduced under reduced pressure affording a brown solid which was washed with several portions of *n*-pentane and dried under reduced pressure for 6 hours. The product was isolated as a brown powder with a yield of 83%. Crystals suitable for X-ray diffraction studies were grown from a saturated fluorobenzene solution using vapor diffusion of *n*-pentane at -8 °C for 2 days. Elemental analysis for $C_{36}H_{47}F_3N_2O_3OsS$: Found (Calculated): C: 52.46 (51.78), H: 5.95 (5.67), N: 3.30 (3.35). ESI-MS (CH_2Cl_2, m/z) positive mode: 685.9914 (100% calculated 685.9910). ^{1}H NMR (25 °C, 400 MHz, CD_2Cl_2), δ(ppm): 1.17 (d, $^3J_{HH}$ = 6.4 Hz, 12H, $CH(CH_3)_2$), 1.39 (d, $^3J_{HH}$ = 4.6 Hz, 12H, $CH(CH_3)_2$), 2.42 (s br., 6H, α-$NCCH_3$), 2.71 (sept, 4H, $CH(CH_3)_2$), 5.89 (s br, 6H, C_6H_6), 6.96 (s br, 1H, β-*CH*), 7.42 (m, 6H, Ar *p*-*CH*). ^{13}C NMR

(25 °C, 100 MHz, CD_2Cl_2), δ(ppm): 23.44 (s, α-NC*C*H$_3$), 24.59 (s, CH(*C*H$_3$)$_2$)$_2$), 25.50 (s, (CH(*C*H$_3$)$_2$), 29.29 (s, *C*H(CH$_3$)$_2$), 76.83 (s, *C*$_6$H$_6$), 106.99 (s, β-*C*H), 124.79 (s, Ar *m*-*C*H), 129.43 (s, Ar *p*-*C*H). ^{19}F NMR (25 °C, 376 MHz, CD_2Cl_2), δ(ppm): -78.87 (SO$_3$C*F*$_3$). UV-Visible (25°C, CH_2Cl_2), λ_{max} (nm) [ε (L mol^{-1} cm^{-1})]: 484 [9.85 × 10^2], 382 [5.14 × 10^3], 302 [1.95 × 10^4].

1,4-Hexyne-η^6-benzene-Ru(II)-β-thioketoiminate tetrakis-3,5-trifluoromethylphenylborate (10): In a dry Schlenk flask, complex 0.090 g of **3c (**0.068 mmol) was dissolved in dry dichloromethane (10 mL) affording a red solution. Anhydrous 1-hexyne (0.15 mL, 1.35 mmol, 10 equivalents) was added dropwise to immediately produce a dark yellow solution. After stirring overnight, the solvent was removed under reduced pressure to give a brown colored residue. The resulting solid was washed with dry *n*-pentane and dried under reduced pressure for 5 hours to afford the product as a pale-yellow powder, total yield 86 %. Elemental analysis for $C_{61}H_{51}F_{14}B_1Ru_1N_1S_1$•0.65$CH_2Cl_2$: Found (Calculated): C: 51.21 (50.96), H: 3.72 (3.63), N: 0.67 (0.96). MS-TOF-ES (positive mode, m/z): 532.7425 (100%, calculated: 532.7446). ^{1}H NMR (25 °C, 400 MHz, CD_2Cl_2), δ(ppm): 0.89–0.90 (m, 3H, C(CH$_2$)$_3$C*H*$_3$), 0.91–0.92 (m, 4H, C(C*H*$_2$)$_3$CH$_3$), 0.93–0.94 (m, 2H, C(C*H*$_2$)$_3$CH$_3$), 1.24-1.26 (m, 6H, Ar *o*-C*H*$_3$), 2.07 (s, 1H, NCC*H*$_3$), 2.14-2.18 (m, 2H, Ar *o*-C*H*CH$_3$), 2.85 (s, 1H, SCC*H*$_3$), 5.60 (s, 6H, C$_6$*H*$_6$), 7.19–7.22 (m, 3H, Ar *p*-C*H*), 7.56 (br s, 4H, *p*-C*H* (BAr^F$_4$)), 7.71 (br s, 8H, *o*-C*H* (BAr^F$_4$)), 9.10 (s, 1H, *H*CC(CH$_2$)$_3$CH$_3$). ^{13}C{^{1}H} NMR (25 °C, 100 MHz, CD_2Cl_2) δ(ppm): 0.72, 13.5, 22.0, 22.8 (NC*C*H$_3$), 24.3, 24.6, 26.3, 27.4, 27.8, 32.2, 36.9, 38.1, 77.3, 94.4 (*C*$_6$H$_6$), 117.4, 123.1, 124.4, 124.6, 125.8, 128.6, 128.8, 134.7, 138.7, 149.4, 162.4 (*C*=S). ^{11}B NMR (128 MHz, 25 °C, CD_2Cl_2) δ ppm: -6.53 (*B*Ar^F$_4$). ^{19}F NMR (376 MHz, 25 °C, CD_2Cl_2) δ(ppm): -62.42 (BAr^F$_4$).

Mono-2,6-Dimethylphenyl isocyanido-η^6-benzene-Ru(II)-β-diketiminate triflate (11): A 50 mL round bottom flask was charged with 0.160 g (0.252 mol) of complex **2a** and completely dissolved with 10 mL of CH_2Cl_2. In a separate 50 mL round bottom flask, 0.036g (0.278 mol, 1.1 equivalent) of 2,6-dimethylphenyl isocyanide (XyNC) was dissolved with 10 mL of CH_2Cl_2. The contents of the second flask was slowly added dropwise to the first flask resulting in a brightly red colored solution. After stirring for 4 hours, all solvent was removed under reduced pressure and the resulting microcrystalline solid washed with 50 mL of *n*-pentane. After the application of vacuum for 14 hours, 0.156 g of a red color solid was obtained representing a yield of 80.7%. A sample suitable for analysis by X-ray diffraction was obtained by the slow diffusion at room temperature of *n*-pentane into a saturated chloroform solution containing **11**. Elemental analysis for $C_{37}H_{40}F_3N_3O_3RuS$•1.3CH_2Cl_2: Found (Calculated): C: 52.66 (52.56), H: 4.81 (4.91), N: 4.80 (4.80). MS-TOF-ESI (CH_2Cl_2), positive mode, (m/z): 616.2996 (100% calculated 616.2266). ^{1}H NMR (25 °C, 400 MHz, CD_2Cl_2), δ(ppm): 1.56 (s, 6H, α-NCC*H*$_3$), 2.24 (s, 6H, o-CC*H*$_3$), 2.34 (s, 6H, o-CC*H*$_3$), 2.59 (s, 6H, o-CC*H*$_3$ (XyNC)), 4.94 (s, 1H, β-C*H*), 5.00 (s, 6H, C$_6$*H*$_6$), 7.14 (m, 3H, Ar *m*-C*H*), 7.24 (d, 3H, Ar *m*-C*H*), 7.35 (m, 3H, Ar *p*-C*H*). ^{13}C NMR (25 °C, 100 MHz, CD_2Cl_2), δ ppm: 18.74 (s, o-C*C*H$_3$), 19.59 (s, o-C*C*H$_3$ (XyNC)), 19.92 (s, o-C*C*H$_3$), 22.72 (s, NC*C*H$_3$), 94.66 (s, *C*$_6$H$_6$), 100.97 (s, β-*C*H), 127.17 (s, Ar *m*-*C*H), 128.08 (s, SO$_3$*C*F$_3$), 129.11 (s, Ar *p*-*C*H), 129.92 (m, Ar *m*-*C*H), 131.89 (s, Ar *i*-*C*CH$_3$), 132.77 (s, Ar *i*-*C*CH$_3$), 136.45 (s, *C*N (XyNC)), 155.67 (s, *i*-*C* (XyNC)), 163.39 (s, α-N*C*CH$_3$). ^{19}F NMR (376 MHz, 25 °C, CD_2Cl_2), δ(ppm): -78.87 (SO$_3$C*F*$_3$). IR (FT-ATR-diamond, 25 °C, solid) υ(cm^{-1}): 3067(w), 2952(w), 2919(w), 2153(br s), 1553(w), 1520(w), 1464(m), 1451(m), 1434(m), 1395(s), 1268(s), 1224(m), 1185(m), 1167(m), 1162(m), 1151(m), 1135(m), 1098(w), 1023(s), 822(m), 774(s), 754(w).

***Tetrakis*-2,6-dimethylphenyl isocyanido-Ru(II)-β-diketiminate triflate (12):** A neck three round-bottom flask equipped with a reflux condenser was charged with 0.322 g (0.512 mmol) of **2a** and dissolved with 10 mL of THF. Subsequently, under a stream of flowing N_2 gas, 0.238 g of solid 2,6-dimethylphenyl isocyanide was added (4.2 equivalents, 2.16 mmol) directly to the reaction mixture. The resulting solution was refluxed at 85 °C for 14 hours. The solvent was removed under reduced pressure and the resulting residue washed with 100 mL of dry *n*-pentane and dried for several hours under reduced pressure. The complex was obtained (0.439 g) as a bright purple powder with a yield of 79%. Elemental Analysis for $C_{54}H_{61}F_3N_6O_3RuS$•$0.71C_5H_{12}$: Found (Calculated): C: 63.37 (63.79), H: 5.96 (4.91), N: 7.25 (7.76). MS-TOF-ESI (positive mode, m/z): 931.2432 (100%, calculated 931.4001). ^{1}H NMR (25 °C, 400 MHz, CD_2Cl_2), δ(ppm): 1.64 (s, 6H, α-NCC*H*$_3$), 2.02 (s, 6H, Ar-C*H*$_3$), 2.36 (s, 12H, Ar-C*H*$_3$), 2.41 (s, 12H, Ar-C*H*$_3$), 5.01 (s, 1H, β-C*H*), 6.95–7.01(m, 6H, Ar *H*), 7.13-7.18 (m, 9H, Ar *H*). ^{13}C NMR (25 °C, 100 MHz, CD_2Cl_2), δ(ppm): 18.6, 19.1, 19.2, 19.4, 19.9, 20.6, 23.4, 98.6, 124.7, 125.7, 128.2, 128.7, 129.0, 129.6, 129.7, 130.5, 1324, 132.7, 135.5, 136.3, 154.6, 163.9. ^{19}F NMR (25 °C, 376 MHz, CD_2Cl_2), δ(ppm): -78.81 (SO_3CF_3). IR (FT-ATR-diamond, 25 °C, solid), υ(cm^{-1}): 2961(w), 2916(w), 21909(w), 2130(s), 2113(s), 1578(w), 1626(w), 1591(w), 1514(m), 1462(m), 1404(m), 1260(s), 1223(m), 1186(m), 1166(m), 1141(m), 1030(m), 1028(s), 921(w), 772(w), 742(m), 718(m), 665(w), 651(w), 636(s), 572(m), 554(w), 545(w), 516(s), 484(m), 435(w).

***Tetrakis*-2,6-diisopropylphenyl isocyanido-Ru(II)-β-thioketoiminate tetrakis-3,5-trifluoro-methylphenylborate (13):** A 100 mL Schlenk flask equipped with a reflux condenser was charged with 0.150 g (0.237 mmol) of complex **7c** and dissolved with 10 mL of THF affording a red-brown colored solution. A separate flask was charged with 0.133 g of dimethyl isocyanide (1.01 mmol, 4.3 equivalents) and dissolved with 5 mL of THF and subsequently added dropwise to the first flask. After refluxing at approximately 85°C overnight, the solvent was removed to give a brownish-yellow residue. The solid was collected and washed with dry *n*-pentane and dried under reduced pressure for several hours affording the product as a pale-brown yellow powder (0.090 g) with a yield of 34%. Elemental Analysis for $C_{69}H_{72}N_5S_1F_{24}B_1Ru$•$0.40CH_2Cl_2$: Found (Calculated): C: 52.05 (51.93), H: 4.44 (4.57), N: 4.22 (4.36). MS-TOF-ESI (positive mode, CH_3CN, m/z): 900.1735 (100 %, calculated: 900.3612). ^{1}H NMR (400 MHz, 25°C, CD_2Cl_2) δ(ppm): 0.99 (d, $^3J_{HH}$ = 6.7 Hz, 3H, CH(C*H*$_3$)$_2$), 1.05 (d, $^3J_{HH}$ = 6.7 Hz, 3H, CH(C*H*$_3$)$_2$), 1.11 (d, $^3J_{HH}$ = 6.7 Hz, 3H, CH(C*H*$_3$)$_2$), 1.16 (d, $^3J_{HH}$ = 6.7 Hz, 3H, CH(C*H*$_3$)$_2$), 1.43 (s, 3H, NCC*H*$_3$), 2.14 (s, 3H, SCC*H*$_3$), 2.24–2.59 (m br, 24H, o-CC*H*$_3$ (XyNC)), 3.38 (sept, $^3J_{HH}$ = 6.7 Hz, 1H, C*H*(CH$_3$)$_2$), 3.85 (sept, $^3J_{HH}$ = 6.7 Hz,1H, C*H*(CH$_3$)$_2$), 6.25 (s, 1H, β-C*H*), 6.97–7.34 (m, 15H, Ar m,p-C*H*) 7.49 (br s, 4H, *p*-C*H* (BAr$^F_4$)), 7.73 (br s, 8H, *o*-C*H* (BAr$^F_4$)). ^{13}C{H} NMR (100 MHz, 25° C, CD_2Cl_2) δ(ppm): 18.19 (s, o-C*C*H$_3$ (XyNC)), 18.27 (s, o-C*C*H$_3$ (XyNC)), 18.27 (s, o-C*C*H$_3$ (XyNC)), 18.36 (s, o-C*C*H$_3$ (XyNC)), 18.72 (s, SC*C*H$_3$), 23.83 (s, CH(*C*H$_3$)$_2$), 23.87 (s, CH(*C*H$_3$)$_2$), 24.53 (s, CH(*C*H$_3$)$_2$), 25.14 (s, CH(*C*H$_3$)$_2$), 28.01 (s, *C*H(CH$_3$)$_2$), 30.03 (s, α-NC*C*H$_3$), 118.34 (s, β-*C*H), 123.49 (s, Ar *C*H), 124.52 (s, Ar *C*H), 125.53 (s, Ar *C*H), 127.34 (s, Ar *C*H), 127.44 (s, Ar *C*H), 127.53 (s, Ar *C*H), 127.75 (Ar *C*H), 128.10 (d, Ar *C*H), 128.39 (s, Ar *C*H), 134.41 (s, *i-C*), 134.76 (s, *i-C*), 134.93 (s, *i-C*), 135.10 (s, *i-C*), 135.16 (s, *i-C*), 153.79 (s, α-N*C*CH$_3$), 167.97 (s, α-S*C*CH$_3$). ^{11}B NMR (128 MHz, 25 °C, CD_2Cl_2) δ ppm: -6.49 (*B*Ar$^F_4$). ^{19}F NMR (376 MHz, 25 °C, CD_2Cl_2) δ(ppm): -62.33 (BAr$^F_4$). IR (FT-ATR-diamond, 25 °C, solid) υ(cm^{-1}): 2962(w), 2921 (w), 2866(w), 2083(br s), 1589(w), 1493(m), 1462(m), 1437(m), 1381(w), 136^{11}B NMR (128 MHz, 25 °C, CD_2Cl_2) δ ppm: -6.53 (*B*Ar$^F_4$)4(w), 1319(w), 1260(s), 1223(m), 1146(m), 1090(s), 1029(s), 934(w), 921(w), 862(w), 797(m), 769(m), 719(m), 668(s), 572(w), 548(m), 513(m), 487(m), 440(m).

^{1}H and $^{13}C\{^{1}H\}$ NMR spectra of **3a** in $CDCl_3$.

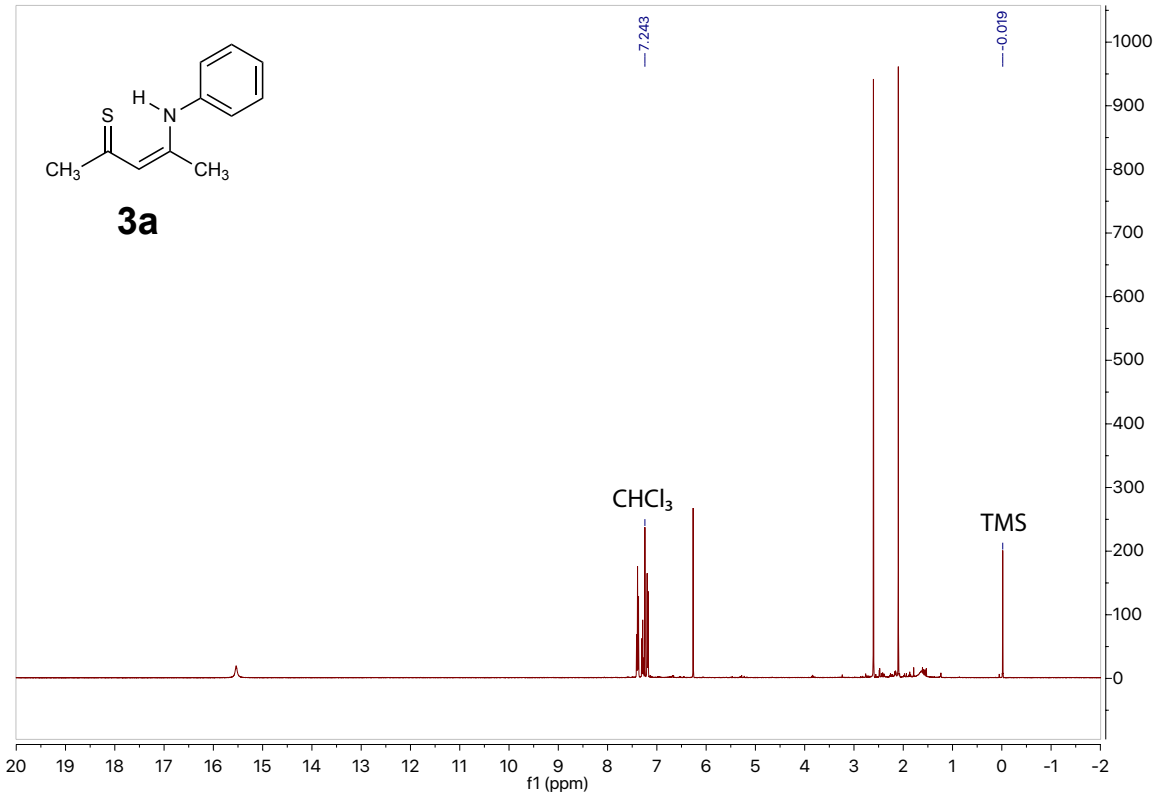

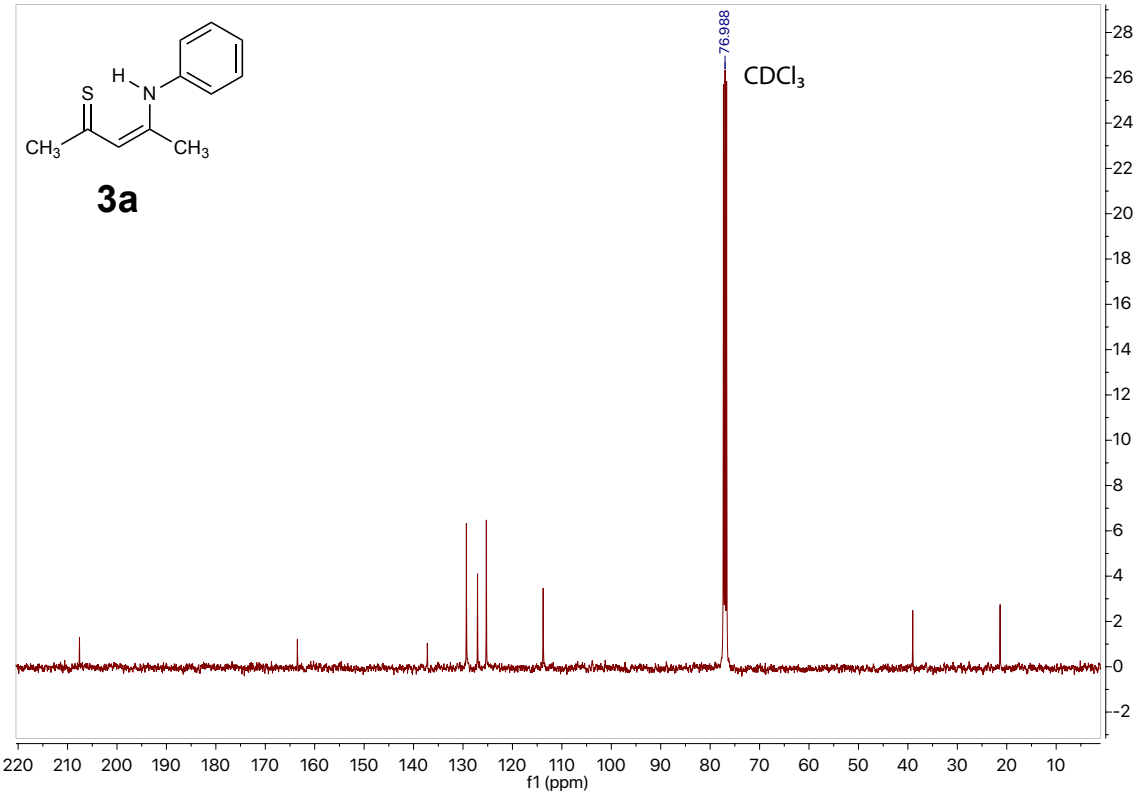

^{1}H NMR spectrum of **4b** in $CDCl_3$.

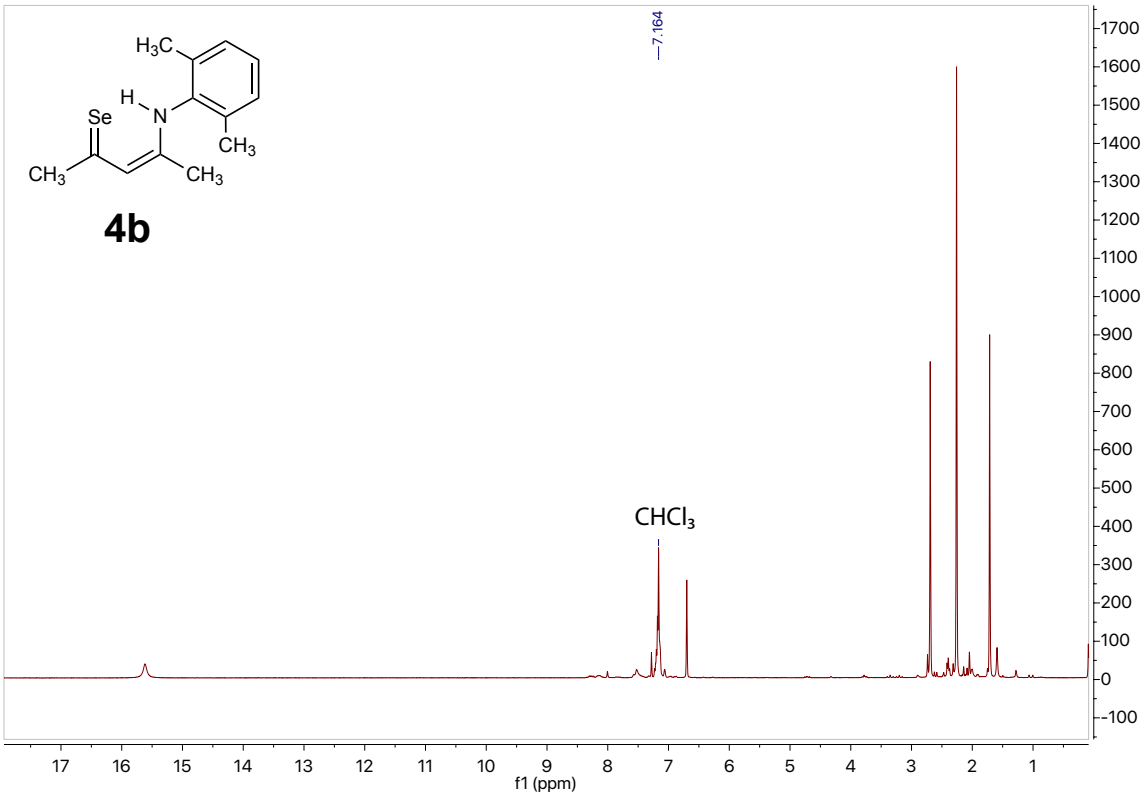

^{1}H and ^{13}C{^{1}H} NMR spectra of **7b[PF$_6$]** in CD_2Cl_2.

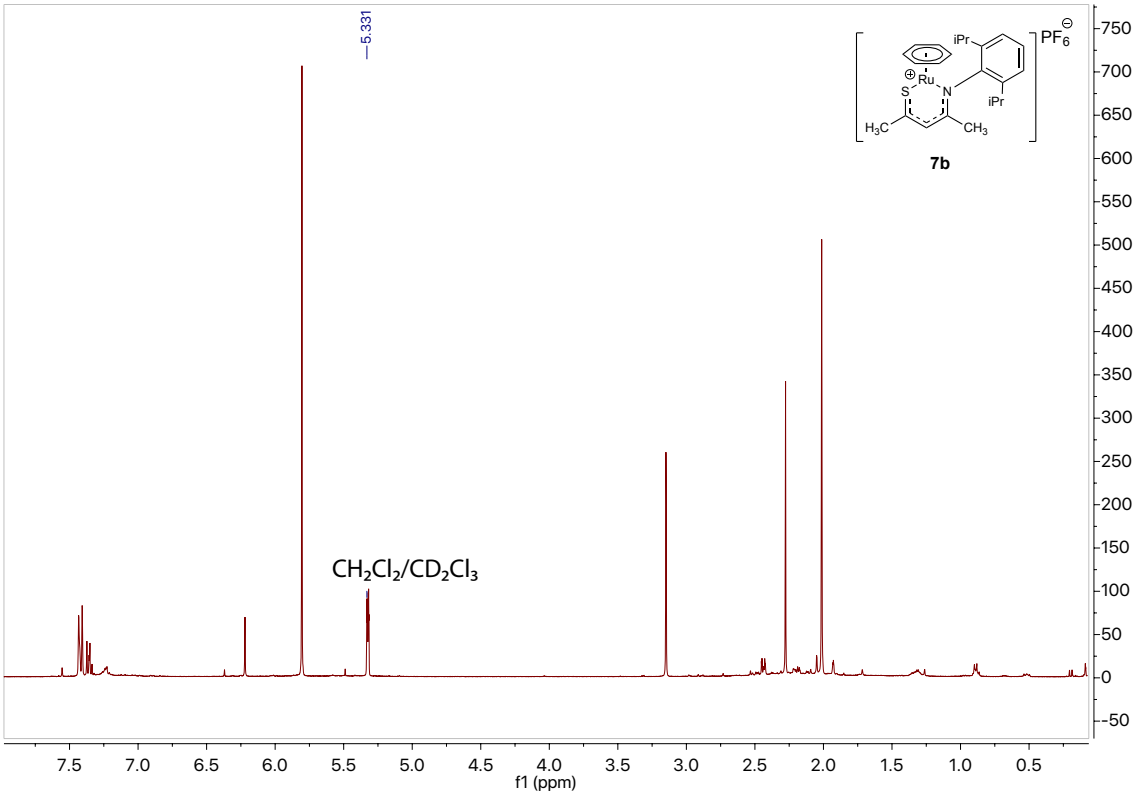

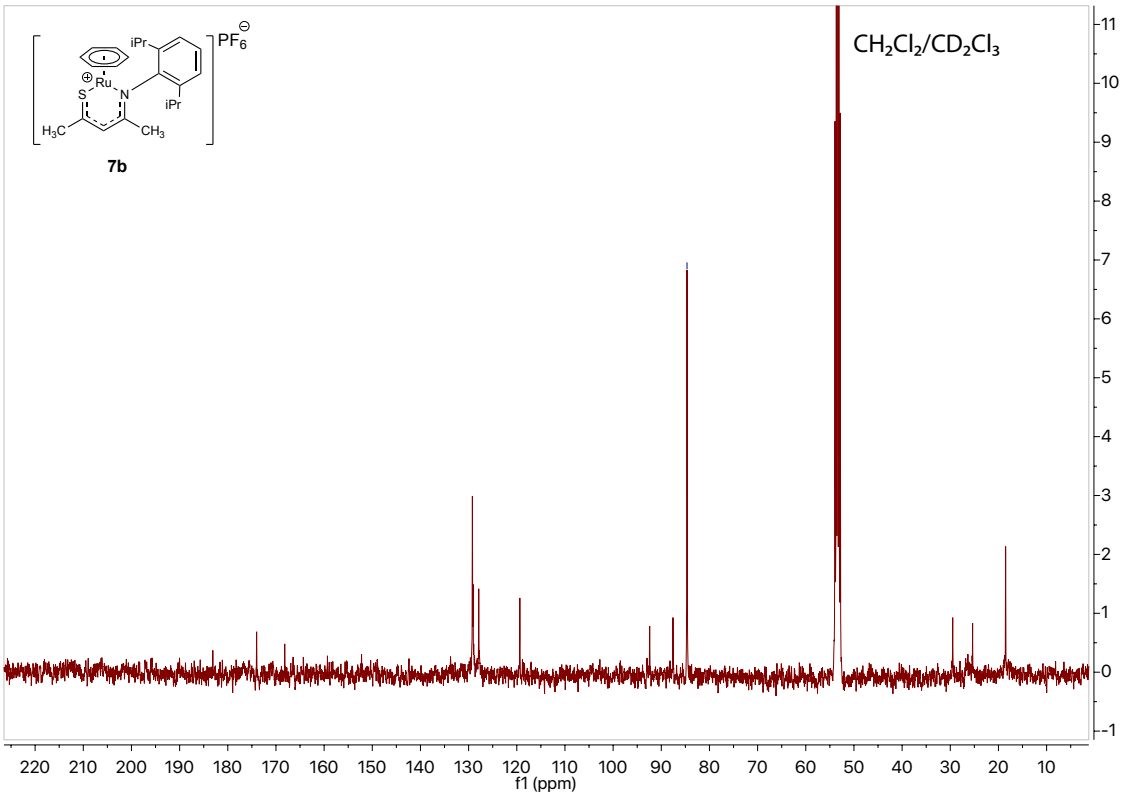

Additional Solid State Structural Information

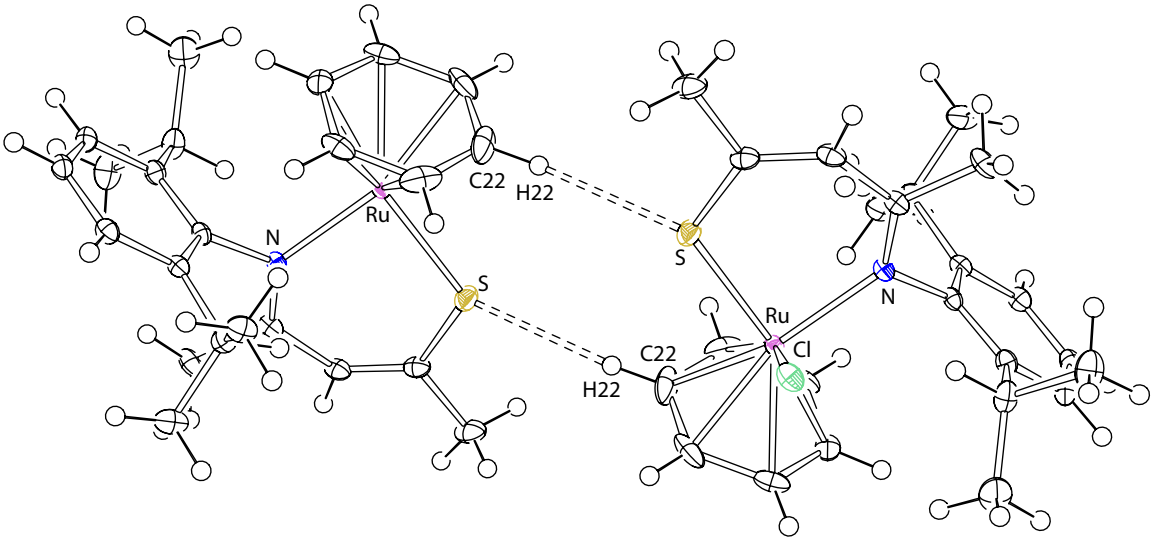

Figure S1: An example of inter-molecular hydrogen bonding in the Ru complex **5c** where the S center of the coordinating β-thioketoiminate is H-bond acceptor with the a hydrogen (H22) atom of a η^6-C_6H_6 ligand of a neighbouring molecule, the distance being 2.754 Å. Analogously, the Os complex **6**, forms an identical hydrogen bonding interaction, with a distance of 2.748 Å. Similarly, **5b** features two hydrogen bonds between the H-accepting S center and H14 of a η^6-arene ligand from neighbouring molecule, and H13A associated with an *ortho*-methyl on *N*-flanking aryl group. Distances between S···H13A is 2.908 Å and S···H14 is 2.964 Å.

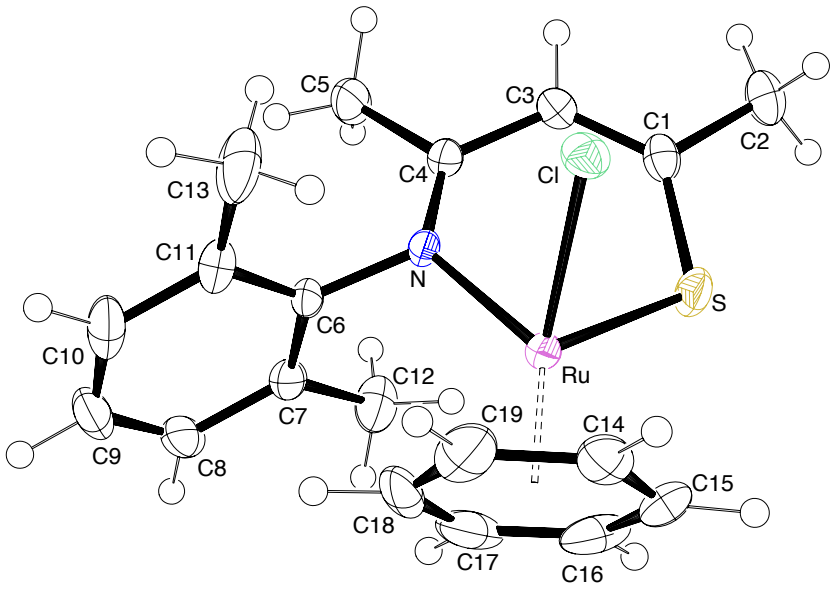

Figure S2: ORTEP representation of **5b**. Thermal ellipsoids are drawn with 50% probability. Selected bond distances (Å) and angles (°): Ru-Cl 2.437 (1); Ru-C_{cent} 1.689 (1); Ru-N 2.142 (1); Ru-S 2.332 (1); S-C1 1.709 (2); N-C4 1.303 (3); S-Ru-N 87.77 (5); C1-C3-C4 127.9 (2); C_{cent}-Ru-N/S_{cent} 147.95 (5); Ru-N/S_{cent}-C13 155.26 (19); Ru-N-C4 130.19 (14); Ru-S-C1 109.79 (7).

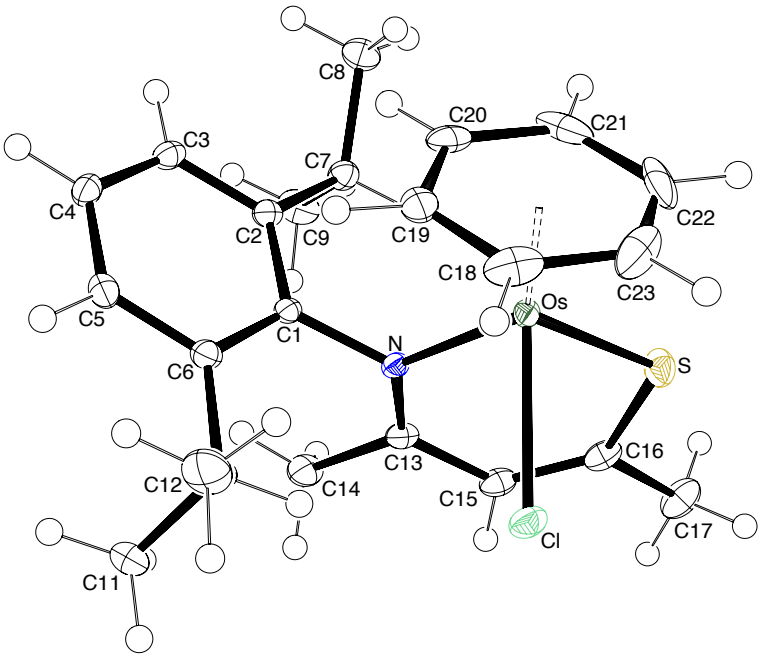

Figure S3: ORTEP representation of **6**. Thermal ellipsoids are drawn with 50% probability. Selected bond distances (Å) and angles (°): Os-Cl 2.443 (4); Os-C_{cent} 1.693 (6); Os-N 2.132 (12); Os-S 2.344 (4); S-C16 1.706 (17); N-C13 1.314 (19); S-Os-N 90.65 (4); C13-C15-C16 130.05 (15); C_{cent}-Os-N/Scent 151.41 (1); Os-N/S_{cent}-C13 154.65 (1); Os-N-C13 128.75 (10); Os-S-C16 111.35 (6).

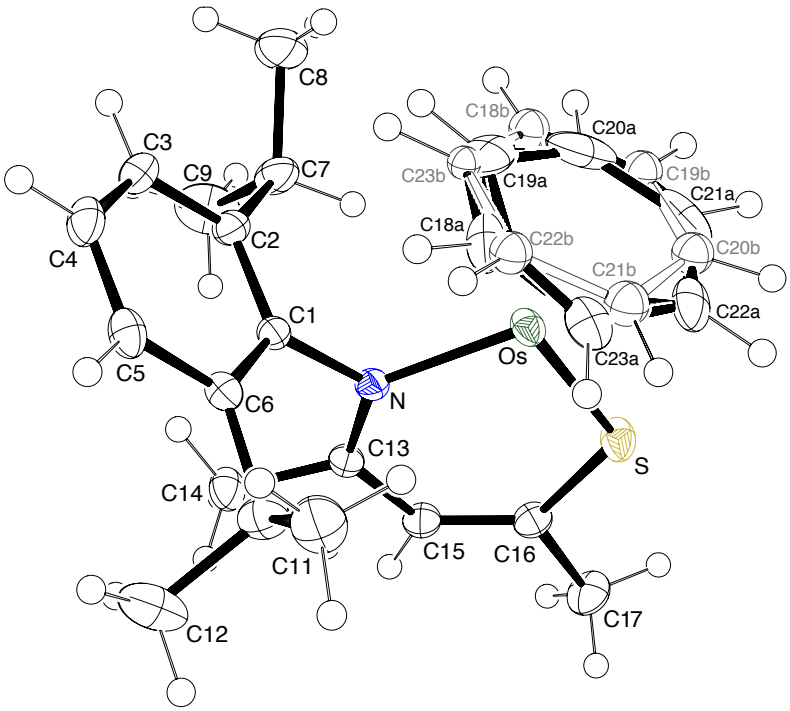

Figure S4: ORTEP representation of the cation of **8**. Thermal ellipsoids are drawn with 50% probability. The anion and solvate have been omitted for clarity. Selected bond distances (Å) and angles (°): Os-C_{cent} 1.702 (1); Os-N 2.025 (14); Os-S 2.227 (5); S-C16 1.702 (19); N-C13 1.339 (2); S-Os-N 94.06 (4); C13-C15-C16 130.48 (17); C_{cent}-Os-N/S_{cent} 171.66 (1); Os-N/S_{cent}-C13 168.13 (1); Os-N-C13 130.69 (12); Os-S-C16 113.69 (6).

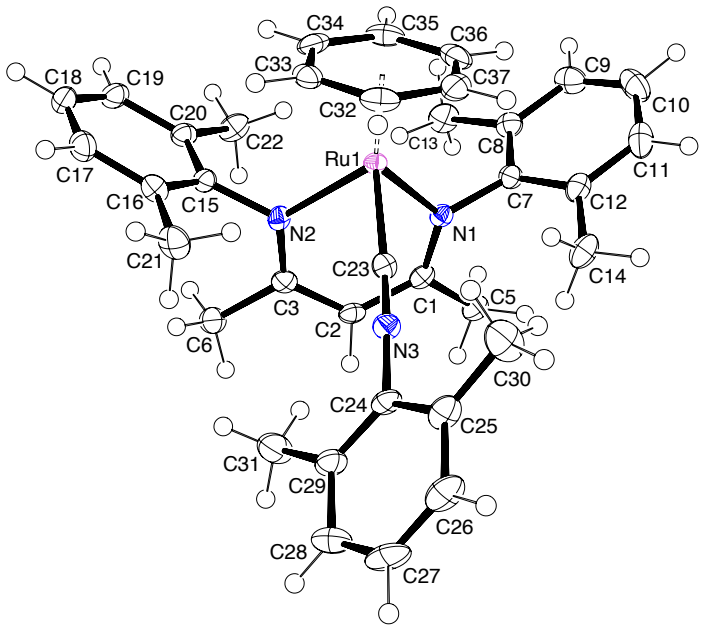

Figure S5: ORTEP representation of the cation of **11**. Thermal ellipsoids are drawn with 50% probability. The anion and solvate have been omitted for clarity. Selected bond distances (Å) and angles (°): Ru-N1 2.098 (2); Ru-N2 2.095 (2); Ru-C23 1.966 (2); Ru-C_{cent} 1.758 (1); N2-C3 1.325 (3); N1-C1 1.318 (3); N1-Ru-N2 87.26 (7); C3-C2-C1 126.0 (2); Ru-C23-N3 175.1 (2); Ru-N1-C1 125.0 (2); Ru-N2-C3 124.0 (2); C_{cen}t-Ru-N/N_{cent} 150.48 (1); Ru-N/N_{cent}-C2 154.20 (1).

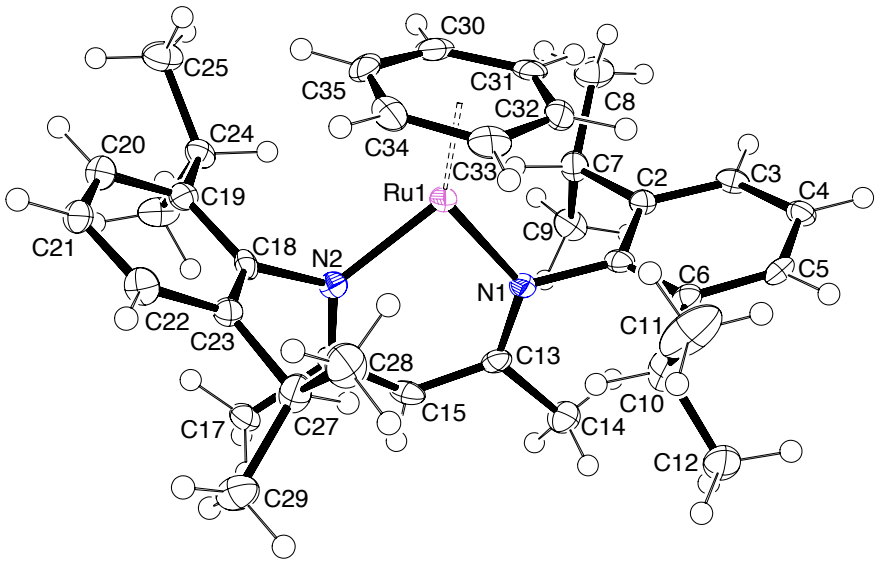

Figure S6: ORTEP representation of the cation of **2c**. Thermal ellipsoids are drawn with 50% probability. The anion and solvate have been omitted for clarity. The unit cell contains two crystallography independent molecules, only one has been drawn. Selected bond distances (Å) and angles (°): Ru-N1 2.020 (4); Ru-N2 2.021 (4); Ru-C_{cent} 1.710 (1); N1-C13 1.351 (6); N2-C16 1.346 (6); N1-Ru-N2 89.9 (2); C13-C15-C16 128.6 (5); Ru-N1-C13 127.9 (3); Ru-N2-C16 127.7 (3); C_{cent}-Ru-N/N_{cent} 179.86 (1); Ru-N/N_{cent}-C15 176.49 (1).

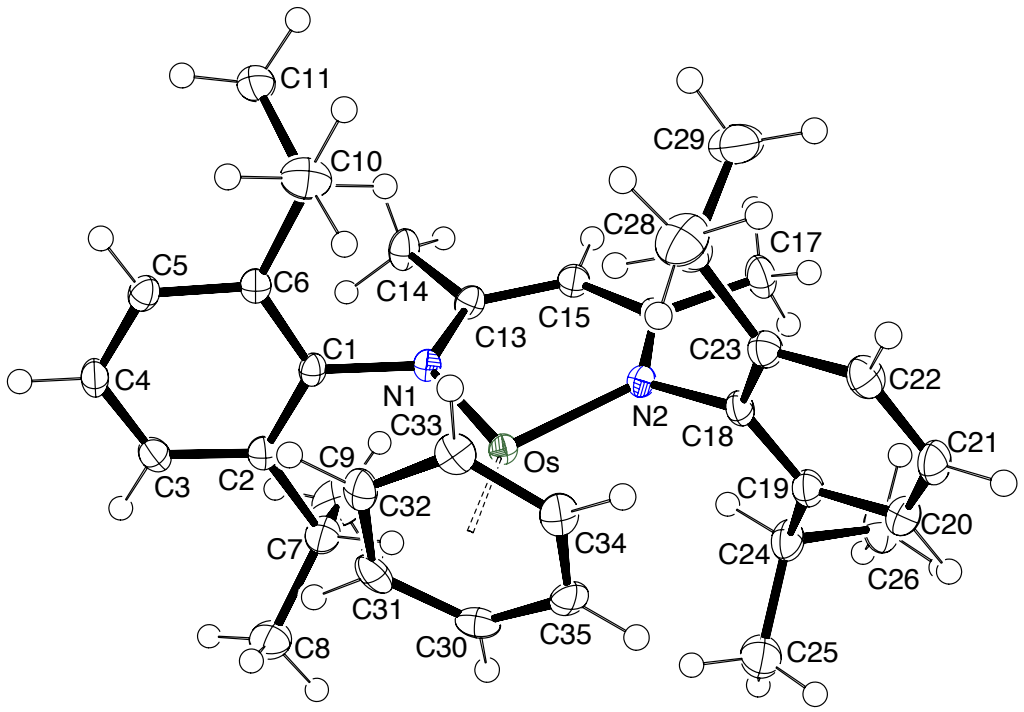

Figure S7: ORTEP representation of the cation of **2d**. Thermal ellipsoids are drawn with 50% probability. The anion and solvate have been omitted for clarity. Selected bond distances (Å) and angles (°): Os-N1 2.009 (1); Os-N2 2.012 (2); Os-C_{cent} 1.701 (1); N1-C13 1.350 (2); N2-C16 1.347 (2); N1-Os-N2 89.73 (6); C13-C15-C16 128.1 (2); Os-N1-C13 127.5 91); Os-N2-C16 128.0 (1); C_{cent}-Os-N/N_{cent} 179.3 (2); Os-N/N_{cent}-C15 177.7 (2).

Specific details on DFT modelling and charge decomposition analysis

Geometry optimizations, Mayer bond indices, molecular and orbital energies were calculated using density functional theory using the Gaussian 09 suite of programs revision e01,[13] on either an Apple Macintosh Pro with 12 cores or the super-computer resource (SGI ICE-X system of 320 nodes) operated by the Irish Center for High End-Computing (ICHEC). Simulated optical absorption spectra were calculated using time-dependent DFT and processed using the AO-MIX program.[14] The three-parameter hybrid meta-gradient-corrected functional (ωB97XD) as developed by Gordon-Head *et al*., (which includes long range dispersion corrections) was employed for all calculations.[15] For each step of the geometry optimizations, self-consistent iterations were performed until a convergence criterion of 10^{-8} was achieved. A double zeta gaussian-type basis set was used and augmented with an additional set of d-orbitals for C, N and an additional p-orbital for hydrogen (6-31G(d,p)).[16] The basis set for sulfur was augmented with two additional sets of d-orbitals (6-31G(2d,p)).[16] The ruthenium and osmium centers were modelled with the SDDAll basis set of double zeta quality, substituting the core electron wave-functions with an effective potential.[17-18] Optimized structures were verified to be stationary minima as indicated by the absence of imaginary frequencies. Where possible, the complexes were symmetry restricted to highest possible point group. Population analysis was performed using Gaussian 09 and the CM5PAC program which employs the charge fitting methodology Charge Model 5 (CM5) developed by Truhlar and Cramer *et al.*[19] Post-quantum analysis including charge decomposition analysis was performed using the AO-MIX suite of programs.[14] Molecular orbital pictures were drawn using Gaussview 6,[20] or the iQmol program (part of the Q-Chem package) developed by Andrew Gilbert.[21]

Table S1: Geometry comparison between DFT (ωB97XD) derived model and experimental solid-state structure of **2c**.

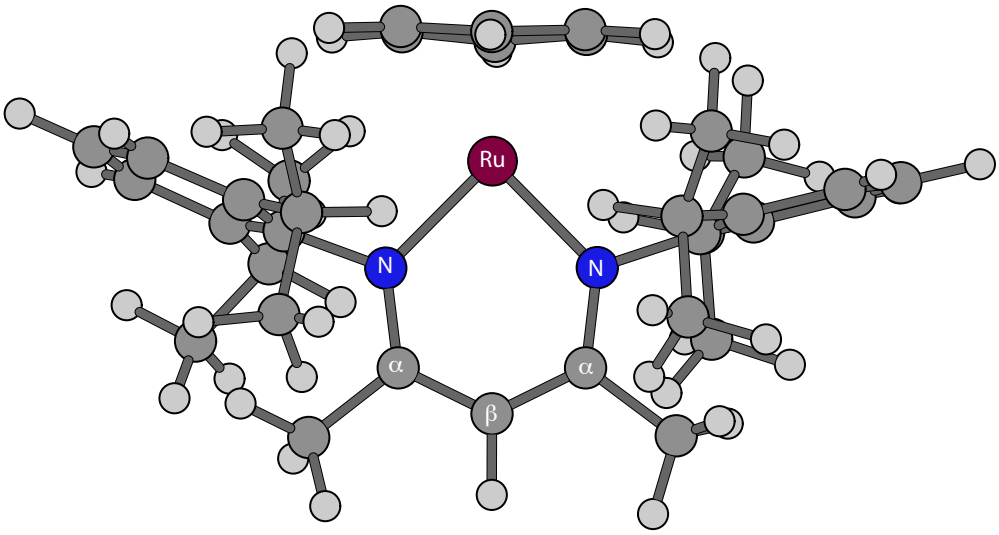

Parameter	Experimental	DFT Calculated	Difference
Bond Distances (Å)			
Ru-N	2.020	2.013	0.007
Ru-N	2.022	2.000	0.021
N-Cα	1.350	1.340	0.010
Cα-Cβ	1.391	1.399	0.008
Cα-Cβ	1.396	1.390	0.006
N-Cα	1.351	1.346	0.005
N-Cipso	1.463	1.445	0.018
N-Cipso	1.468	1.442	0.026
Ru-Arene Centroid	1.708	1.715	0.008
Bond Angles (º)			
N-Ru-N	89.95	89.21	0.74
Ru-N-Cα	127.59	128.30	0.72
N-Cα-Cβ	123.08	123.12	0.04
Cα-Cβ-Cα	128.71	127.72	0.99
N-Cα-Cβ	122.84	122.78	0.06
Ru-N-Cα	127.69	128.83	**1.14**
Ru-N-Cipso	116.80	116.31	0.48
Ru-N-Cipso	116.31	114.63	**1.68**
Arene-Ru-N	135.09	134.88	0.21
Arene-Ru-N	134.95	135.93	0.99

Table S2: Geometry comparison between DFT (ωb97XD) derived model and experimental solid-state structure of **2d**.

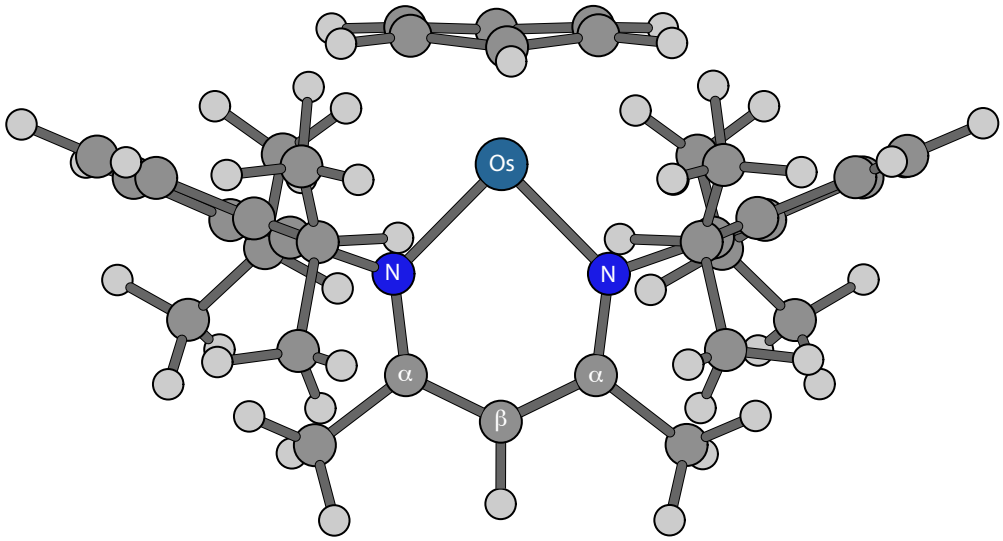

Parameter	Experimental	DFT Calculated	Difference
Bond Distances (Å)			
Os-N	2.009	2.017	0.008
Os-N	2.012	2.017	0.005
N-Cα	1.350	1.345	0.005
Cα-Cβ	1.347	1.391	0.044
Cα-Cβ	1.385	1.391	0.006
N-Cα	1.388	1.345	0.043
N-Cipso	1.460	1.449	0.011
N-Cipso	1.460	1.449	0.011
Os-Arene Centroid	1.701	1.723	0.022
Bond Angles (º)			
N-Os-N	89.73	89.10	0.63
Os-N-Cα	127.53	128.35	0.82
N-Cα-Cβ	123.57	123.15	0.42
Cα-Cβ-Cα	128.06	127.85	0.21
N-Cα-Cβ	123.00	123.17	0.17
Os-N-Cα	128.01	128.33	0.32
Os-N-Cipso	116.70	115.10	**1.60**
Os-N-Cipso	116.44	115.15	**1.29**
Arene-Os-N	135.36	135.40	0.04
Arene-Os-N	134.90	135.41	0.51

Table S3: Geometry comparison between DFT (ωB97XD) derived model and experimental solid-state structure of **7c**.

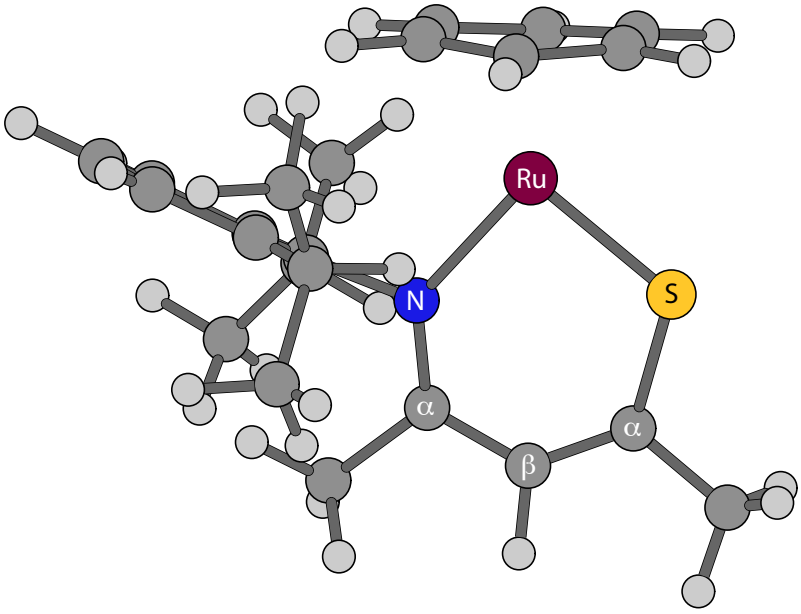

Parameter	Experimental	DFT Calculated	Difference
Bond Distances (Å)			
Ru-N	2.035	2.055	0.020
Ru-S	2.213	2.237	0.024
N-Cα	1.329	1.326	0.003
Cα-Cβ	1.419	1.423	0.004
Cα-Cβ	1.359	1.366	0.007
C-Sα	1.695	1.711	0.016
N-Cipso	1.460	1.450	0.010
Ru-Arene Centroid	1.692	1.714	0.022
Bond Angles (º)			
N-Ru-S	94.15	93.07	**1.08**
Ru-N-Cα	130.33	131.61	**1.28**
N-Cα-Cβ	125.53	125.46	0.07
Cα-Cβ-Cα	131.04	130.41	0.63
S-Cα-Cβ	125.01	125.56	0.55
Ru-S-Cα	113.88	113.87	0.01
Ru-N-Cipso	113.55	111.52	**2.03**
Arene-Ru-N	137.9	136.94	0.96
Arene-Ru-S	127.93	129.99	**2.06**

Table S4: Geometry comparison between DFT (ωB97XD) derived model and experimental solid-state structure of **8**.

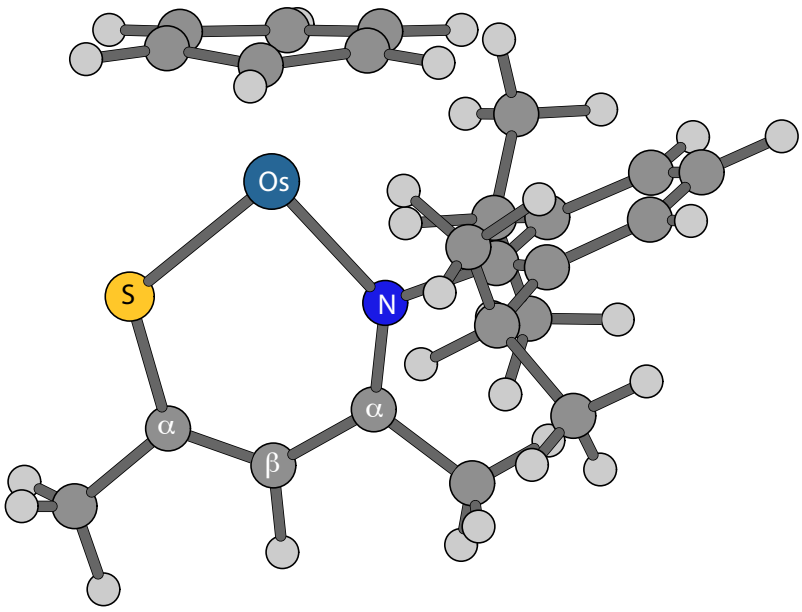

Parameter	Experimental	DFT Calculated	Difference
Bond Distances (Å)			
Os-N	2.025	2.051	0.026
Os-S	2.227	2.255	0.028
N-Cα	1.339	1.332	0.007
Cα-Cβ	1.415	1.420	0.005
Cα-Cα	1.369	1.367	0.002
N-S	1.702	1.710	0.008
N-Cipso	1.460	1.454	0.006
Os-Arene Centroid	1.702	1.721	0.019
Bond Angles (º)			
N-Os-S	94.07	93.31	0.76
Os-N-Cα	130.63	131.15	0.52
N-Cα-Cβ	125.89	125.86	0.03
Cα-Cβ-Cα	130.48	130.66	0.18
S-Cα-Cβ	125.2	125.56	0.36
Os-S-Cα	113.69	113.45	0.24
Os-N-Cipso	113.62	112.36	**1.26**
Arene-Os-N	137.63	136.44	**1.19**
Arene-Os-S	128.13	130.24	**2.11**

Table S5: Atomic charge comparison using the Hirshfeld and CM5 population analysis schemes for the cationic Ru and Os complexes bearing β-diketiminate or β-thioketoiminate ligand bearing the *N*-2,6-diisopropylphenyl substituent, **2c-d**, **7c** and **8**.

	2c M = Ru, E = N		**2d** M = Os, E = N		**7c** M = Ru, E = S		**8** M = Os, E = S	
	Hirshfeld	**CM5**	**Hirshfeld**	**CM5**	**Hirshfeld**	**CM5**	**Hirshfeld**	**CM5**
C(Arene)	-0.0172	-0.1046	-0.0107	-0.0974	-0.0112	-0.0977	-0.0035	-0.0893
C(Arene)	-0.0157	-0.1032	-0.0086	-0.0957	-0.0108	-0.0963	-0.0039	-0.0887
C(Arene)	-0.0174	-0.1108	-0.0107	-0.1045	-0.0101	-0.1035	-0.0021	-0.0956
C(Arene)	-0.0159	-0.1097	-0.0090	-0.1034	-0.0102	-0.1033	-0.0022	-0.0953
C(Arene)	-0.0165	-0.1049	-0.0105	-0.0973	-0.0106	-0.0995	-0.0036	-0.0912
C(Arene)	-0.0153	-0.1038	-0.0087	-0.0956	-0.0081	-0.0978	-0.0006	-0.0891
M	0.3220	0.8032	0.2065	0.6777	0.2712	0.6858	0.1512	0.5594
E	-0.0954	-0.3968	-0.0729	-0.3716	-0.0569	-0.1619	-0.0193	-0.1205
N	-0.0965	-0.4011	-0.0729	-0.3716	-0.0846	-0.3759	-0.0610	-0.3515
α-C(N)	0.0925	0.1471	0.0948	0.1491	0.0338	0.0325	0.0352	0.0339
β-C	-0.0875	-0.1317	-0.0901	-0.1343	-0.0649	-0.1124	-0.0661	-0.1136
α-C(N/S)	0.0932	0.1485	0.0947	0.1490	0.1113	0.1689	0.1131	0.1696

Table S6: CDA-based comparison of forward and backward charge donation (CT) for cationic η^6-arene-Ru and -Os complexes supported by β-diketiminate (NacNac, top) or β-thioketoiminate (NacTac, bottom) ligands. Values are totals from the combination of α and β spins.

Symmetry/ bond type	**Ru**		**Os**	
	$NacNac^{-1} \rightarrow [C_6H_6Ru]^{2+}$ Forward CT	$NacNac^{-1} \leftarrow [C_6H_6Ru]^{2+}$ Backward CT	$NacNac^{-1} \rightarrow [C_6H_6Os]^{2+}$ Forward CT	$NacNac^{-1} \leftarrow [C_6H_6Os]^{2+}$ Backward CT
A_1 (σ)	0.246	0	0.226	0
B_2 (σ)	0.292	0	0.222	0
B_1 (π)	0.304	0	0.31	0
A_2 (π)	0.056	0.034	0.054	0.042
σ-total	0.538	0	0.448	0
π-total	0.360	0.034	0.364	0.042
Total	0.898	0.034	0.814	0.042

Symmetry/ bond type	**Ru**		**Os**	
	$NacTac^{-1} \rightarrow [C_6H_6Ru]^{2+}$ Forward CT	$NacTac^{-1} \leftarrow [C_6H_6Ru]^{2+}$ Backward CT	$NacTac^{-1} \rightarrow [C_6H_6Os]^{2+}$ Forward CT	$NacTac^{-1} \leftarrow [C_6H_6Os]^{2+}$ Backward CT
A' (σ)	0.662	0.042	0.612	0.034
A'' (π)	0.336	0.046	0.346	0.054
Total	0.998	0.088	0.958	0.088

Table S7: CDA-based comparison of forward and backward charge donation (CT) for the cationic η^6-arene-Ru and -Os complexes supported by β-diketiminate (NacNac) or β-thioketoiminate (NacTac) ligands. Values are totals from the combination of α and β spins.

Forward Donation		**Back Donation**		**Forward/back (f/b) CT ratio**
$RuNacNac^{+1} \rightarrow [C_6H_6]$	1.109	$RuNacNac^{+1} \leftarrow [C_6H_6]$	0.520	2.13
$OsNacNac^{+1} \rightarrow [C_6H_6]$	1.069	$OsNacNac^{+1} \leftarrow [C_6H_6]$	0.555	1.93
$RuNacTac^{+1} \rightarrow [C_6H_6]$	0.950	$RuNacTac^{+1} \leftarrow [C_6H_6]$	0.426	2.23
$OsNacTac^{+1} \rightarrow [C_6H_6]$	0.954	$OsNacTac^{+1} \leftarrow [C_6H_6]$	0.488	1.95

Figure S8: Selected MOs composition of the LUMOs+2 to HOMO-14 of the cationic η^6-C_6H_6 Ru β-diketiminate complex with *N*-phenyl substituents.

$[(\eta^6\text{-}C_6H_6)\text{RuNacNac(Ph)}]^+$ MOs LUMO+2 to HOMO-2

LUMO+2	**LUMO+1**	**LUMO**
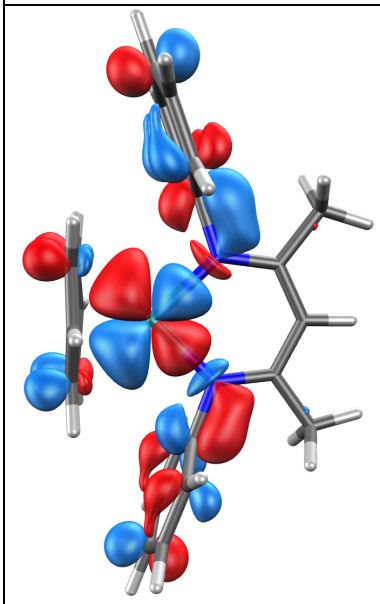 B_2	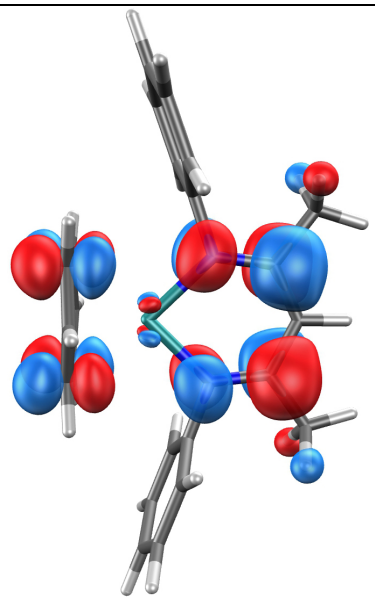 A_2	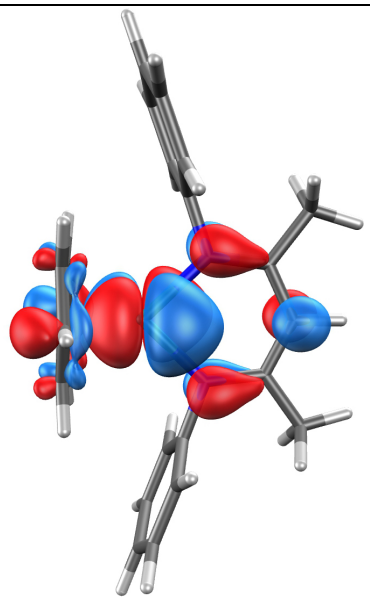 B_1
Ru: 41.44% Arene: 13.06% NacNac: 45.49%	Ru: 0.40% Arene: 26.74% NacNac: 72.86%	Ru: 60.23% Arene: 19.34% NacNac: 20.43%
HOMO	**HOMO-1**	**HOMO-2**
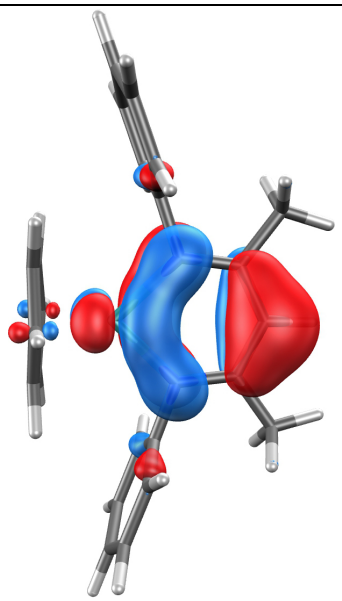 **B_1**	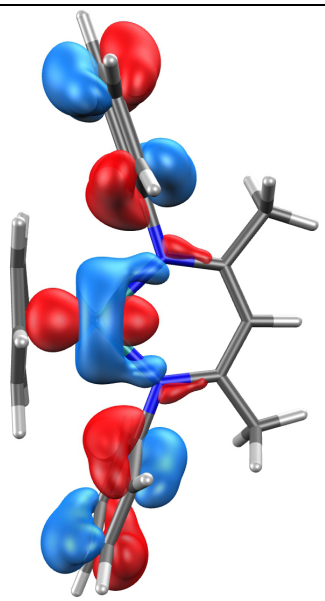 **A_1**	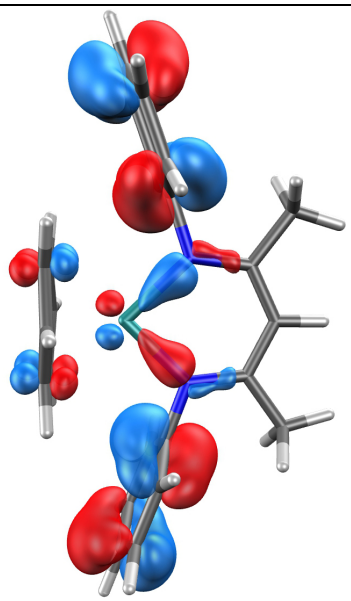 **B_2**
Ru: 10.45% Arene: 5.30% NacNac: 82.25%	Ru: 15.88% Arene: 1.25% NacNac: 82.86%	Ru: 1.47% Arene: 7.99% NacNac: 90.54%

$[(\eta^6\text{-}C_6H_6)RuNacNac(Ph)]^+$ MOs HOMO-3 to HOMO-8

HOMO-3	HOMO-4	HOMO-5
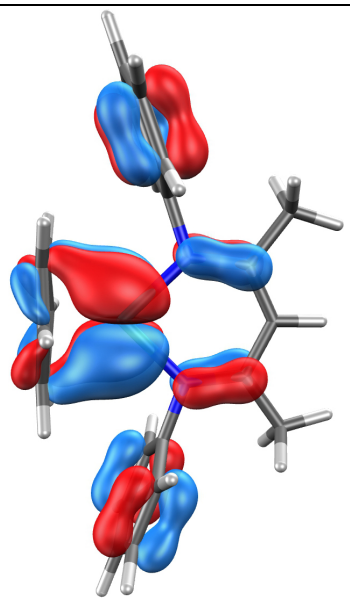 A_2	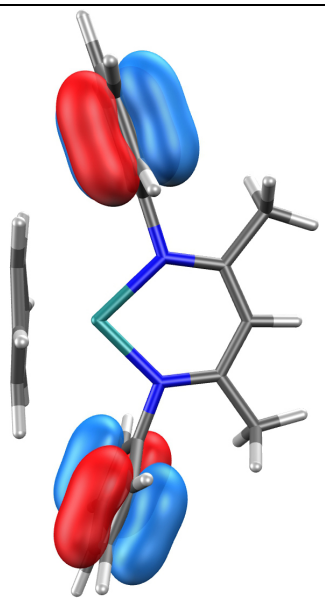 B_1	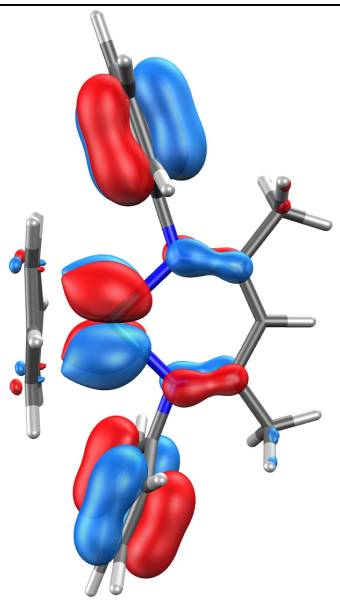 A_2
Ru: 44.22% Arene: 9.56% NacNac: 47.23%	Ru: 0.28% Arene: 1.12% NacNac: 98.59%	Ru: 16.65% Arene: 4.85% NacNac: 78.49%
HOMO-6	**HOMO-7**	**HOMO-8**
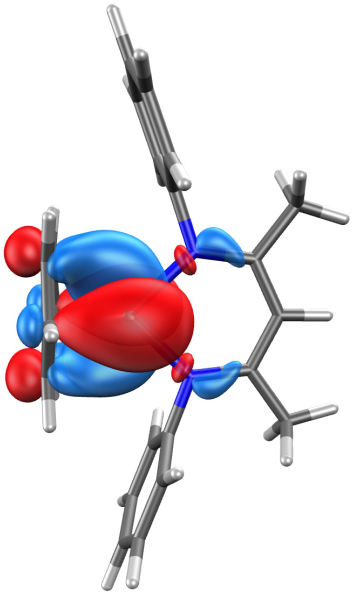	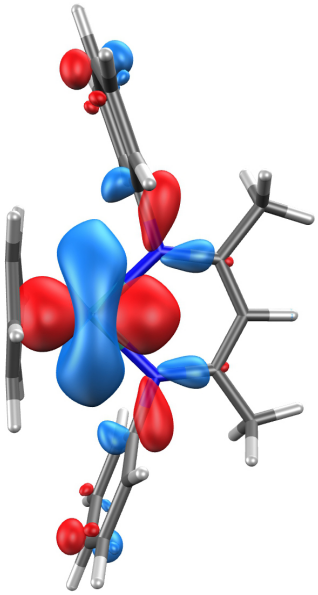	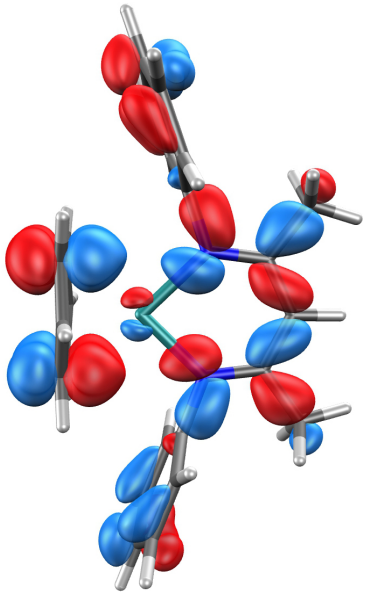
Ru: 69.75% Arene: 19.49% NacNac: 10.76%	Ru: 71.84% Arene: 5.48% NacNac: 22.68%	Ru: 3.67% Arene: 32.74% NacNac: 63.59%

$[(\eta^6\text{-}C_6H_6)RuNacNac(Ph)]^+$ MOs HOMO-9 to HOMO-14

HOMO-9	HOMO-10	HOMO-11
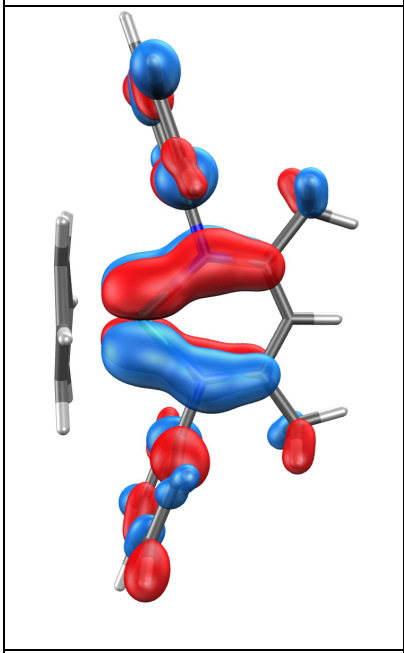	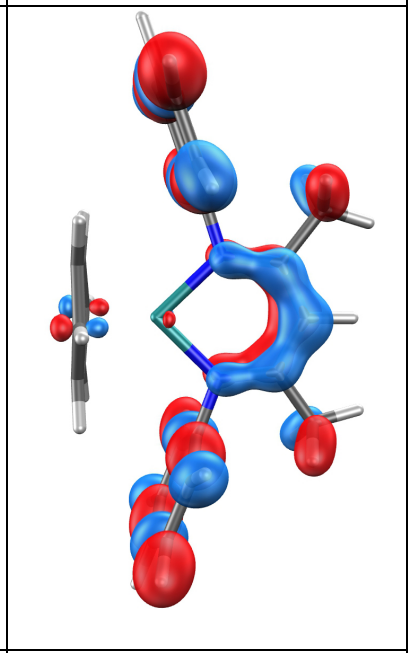	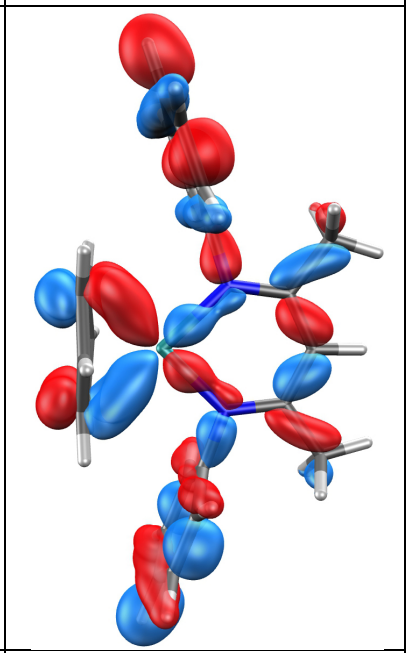
Ru: 17.35% Arene: 3.07% NacNac: 79.58%	Ru: 1.47% Arene: 4.57% NacNac: 93.96%	Ru: 6.25% Arene: 19.41% NacNac: 74.35%
HOMO-12	**HOMO-13**	**HOMO-14**
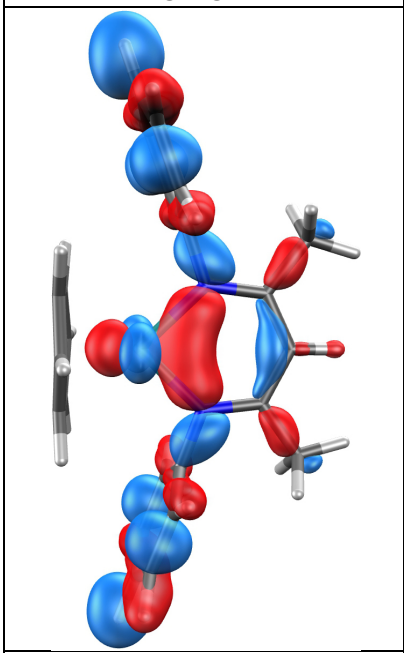	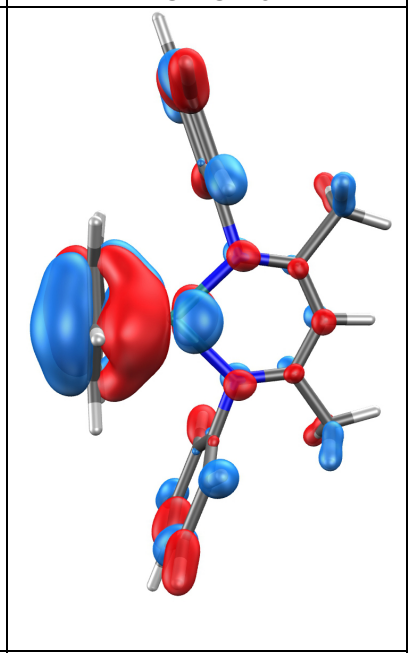	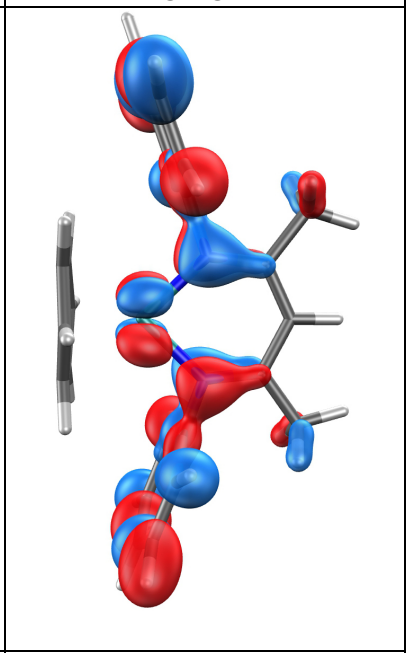
Ru: 6.13% Arene: 1.78% NacNac: 92.09%	Ru: 12.37% Arene: 51.14% NacNac: 36.50%	Ru: 3.53% Arene: 1.43% NacNac: 95.03%

Figure S9: MOs composition of the LUMOs+2 to HOMO-16, HOMO-18 of the cationic η^6-C_6H_6 Ru β-thioketoiminate complex with a *N*-phenyl substituent.

$[(\eta^6\text{-}C_6H_6)\text{RuNacTac(Ph)}]^+$ MOs LUMO+2 to HOMO-2

LUMO+2	**LUMO+1**	**LUMO**
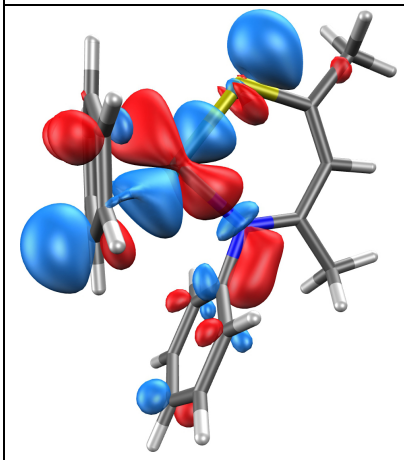 A’	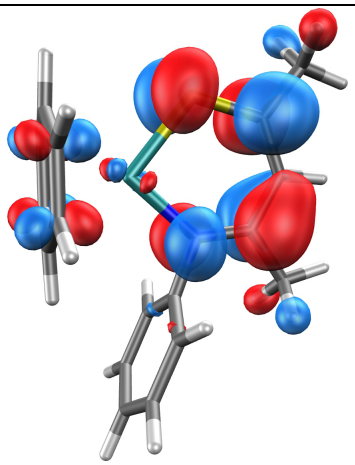 A”	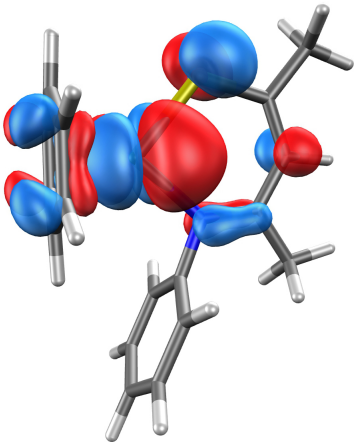 A”
Ru: 42.17% Arene: 22.33% NacTac: 34.51%	Ru: 0.97% Arene: 11.32% NacTac: 87.72%	Ru: 60.06% Arene: 19.25% NacTac: 20.69%
HOMO	**HOMO-1**	**HOMO-2**
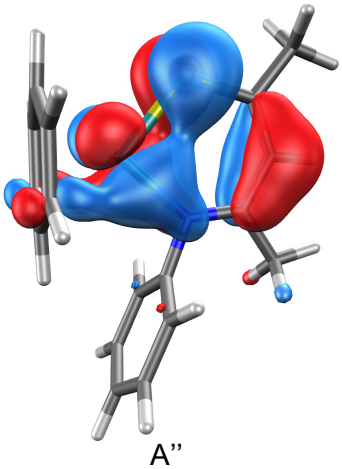 A”	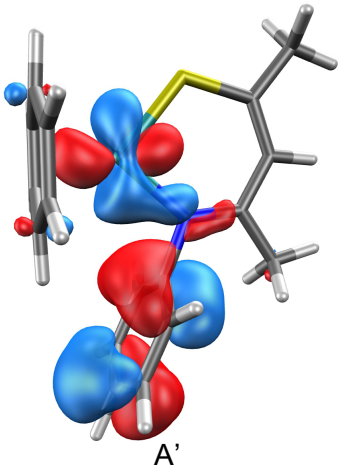 A’	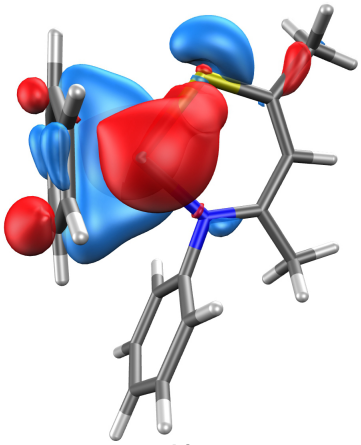 A’
Ru: 20.48% Arene: 7.65 % NacTac: 71.88%	Ru: 12.48% Arene: 4.74% NacTac: 82.78%	Ru: 63.40% Arene: 14.86% NacTac: 21.73%

$[(\eta^6\text{-}C_6H_6)RuNacTac(Ph)]^+$ MOs HOMO-3 to HOMO-8

HOMO-3	HOMO-4	HOMO-5
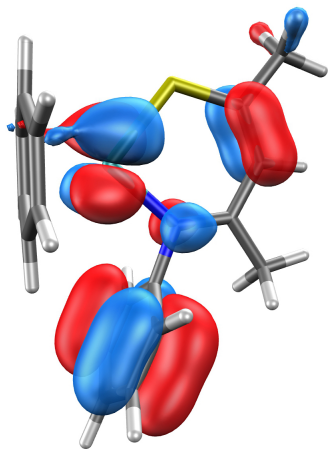 A”	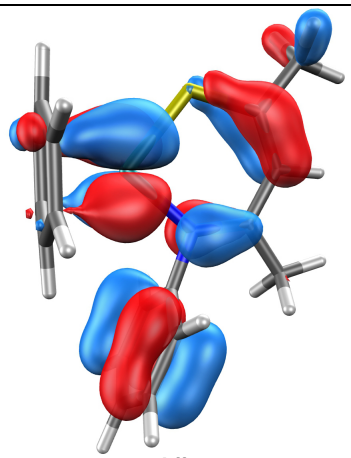 A”	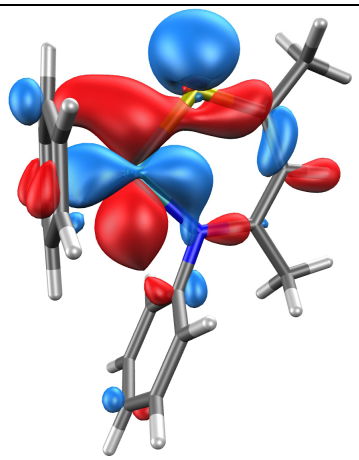 A’
Ru: 13.44% Arene: 3.34% NacTac: 83.21%	Ru: 23.59% Arene: 7.13% NacTac: 69.29%	Ru: 51.07% Arene: 9.19% NacTac: 39.74%
HOMO-6	**HOMO-7**	**HOMO-8**
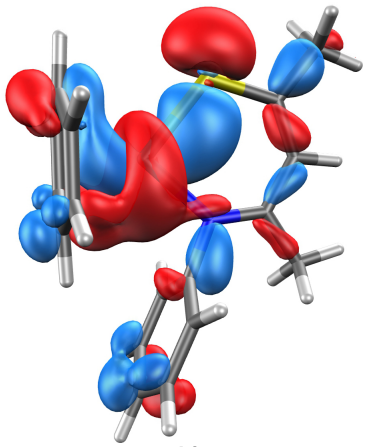 A’	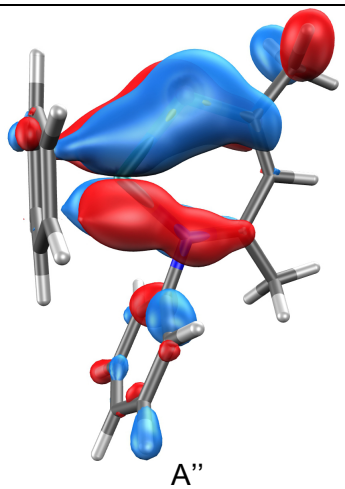 A”	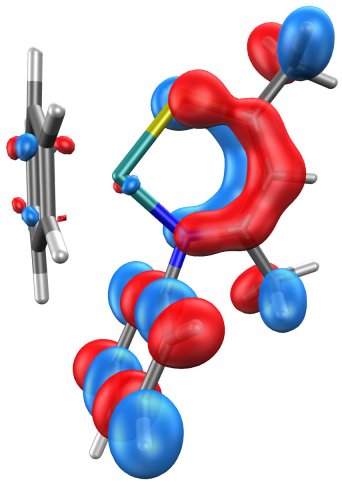 A”
Ru: 31.14% Arene: 18.00% NacTac: 50.85%	Ru: 30.79% Arene: 5.82% NacTac: 63.39%	Ru: 1.85% Arene: 5.19% NacTac: 92.96%

$[(\eta^6\text{-}C_6H_6)RuNacTac(Ph)]^+$ MOs HOMO-9 to HOMO-14

HOMO-9	HOMO-10	HOMO-11
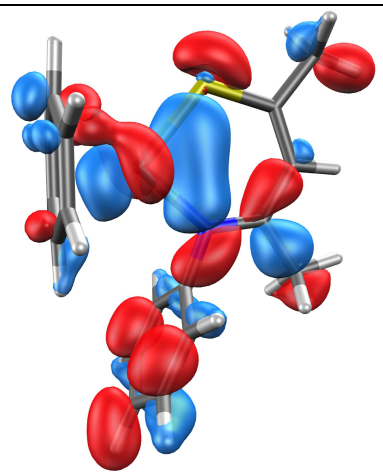 A’	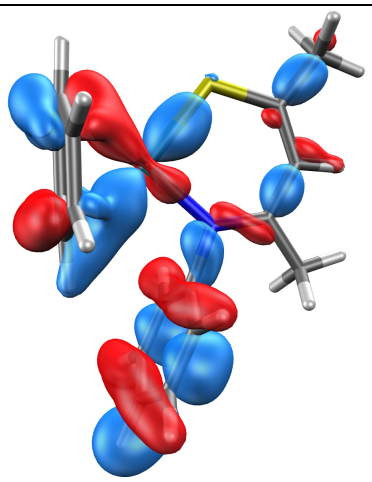 A’	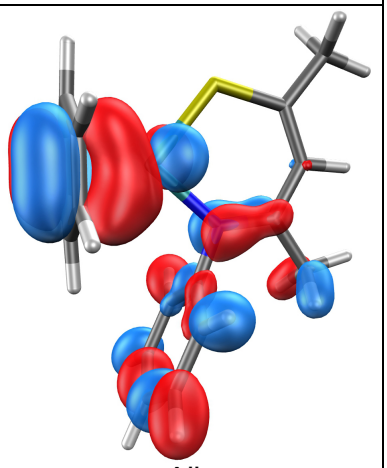 A”
Ru: 14.72% Arene: 10.27% NacTac: 75.01%	Ru: 7.71% Arene: 21.16% NacTac: 71.12%	Ru: 12.06% Arene: 44.67% NacTac: 43.27%
HOMO-12	**HOMO-13**	**HOMO-14**
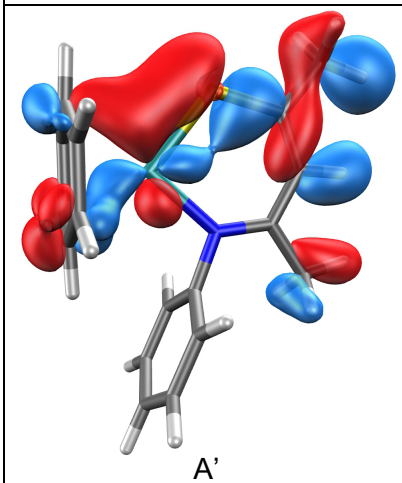 A’	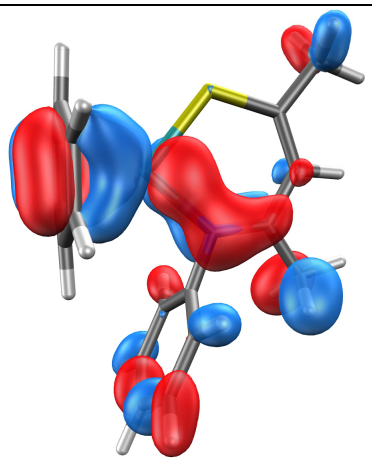 A”	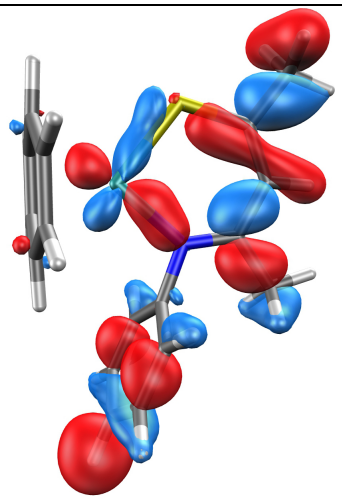 A’
Ru: 9.17% Arene: 14.89% NacTac: 75.94%	Ru: 13.97% Arene: 27.37% NacTac: 58.66%	Ru: 3.40% Arene: 3.49% NacTac: 93.02%

$[(\eta^6\text{-}C_6H_6)RuNacTac(Ph)]^+$ MOs HOMO-15 to HOMO-16, HOMO-18

HOMO-15	HOMO-16	HOMO-18
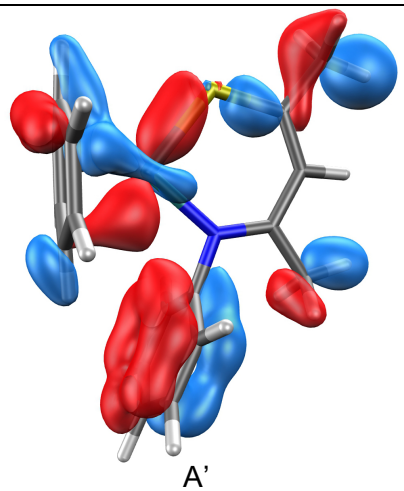 A’	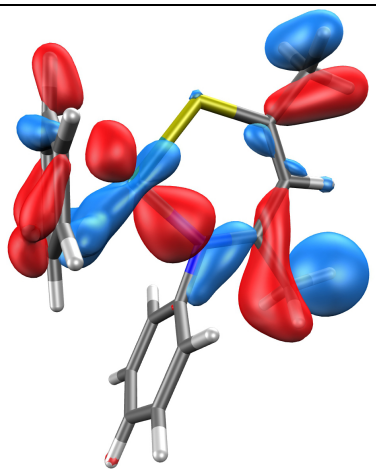 A’	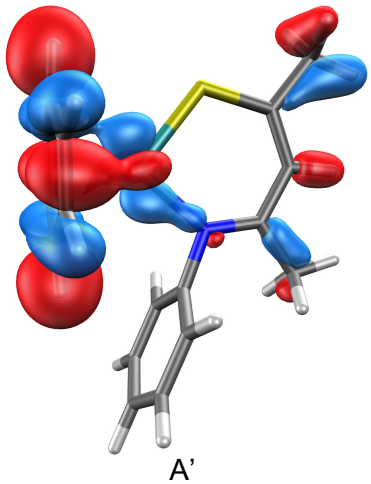 A’
Ru: 7.50% Arene: 16.02% NacTac: 76.48%	Ru: 8.06% Arene: 15.23% NacTac: 76.71%	Ru: 3.35% Arene: 80.01% NacTac: 16.64%

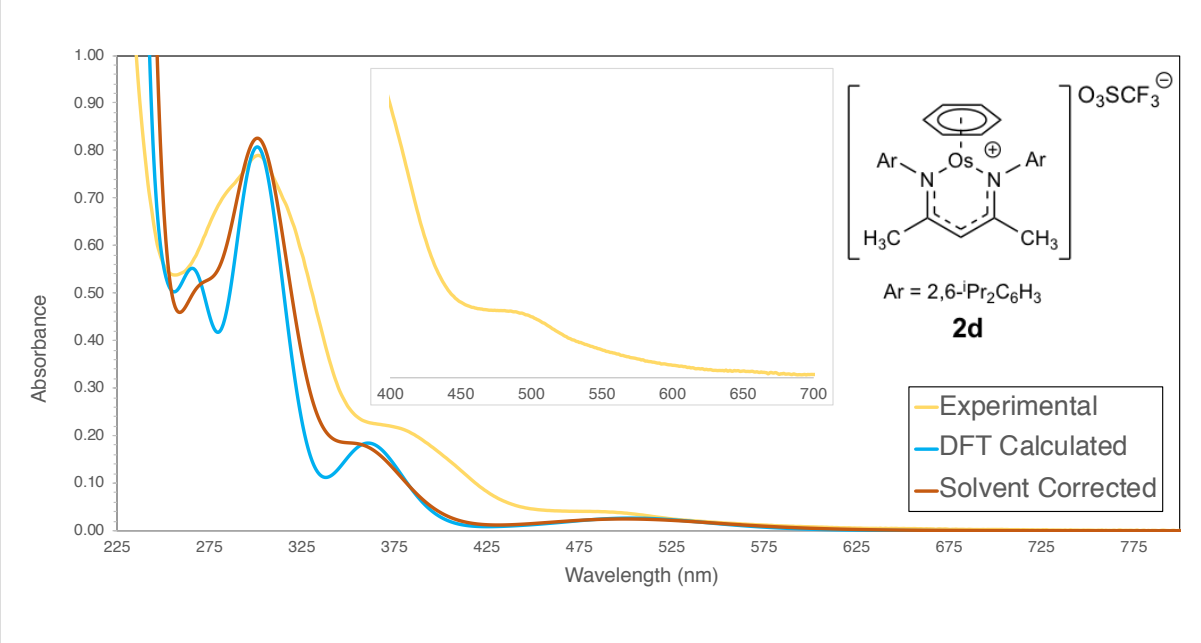

Figure S10: Comparison of experimental (CH_2Cl_2), TD-DFT (ωB97XD, gas phase) and TD-DFT (ωB97XD, CPCM-CH_2Cl_2 corrected) optical absorption spectra for cationic η^6-C_6H_6 Os *N*-2,6-diisopropyl-phenyl-β-diketiminate. The inset shows the weak and board experimental absorption at 484 nm.

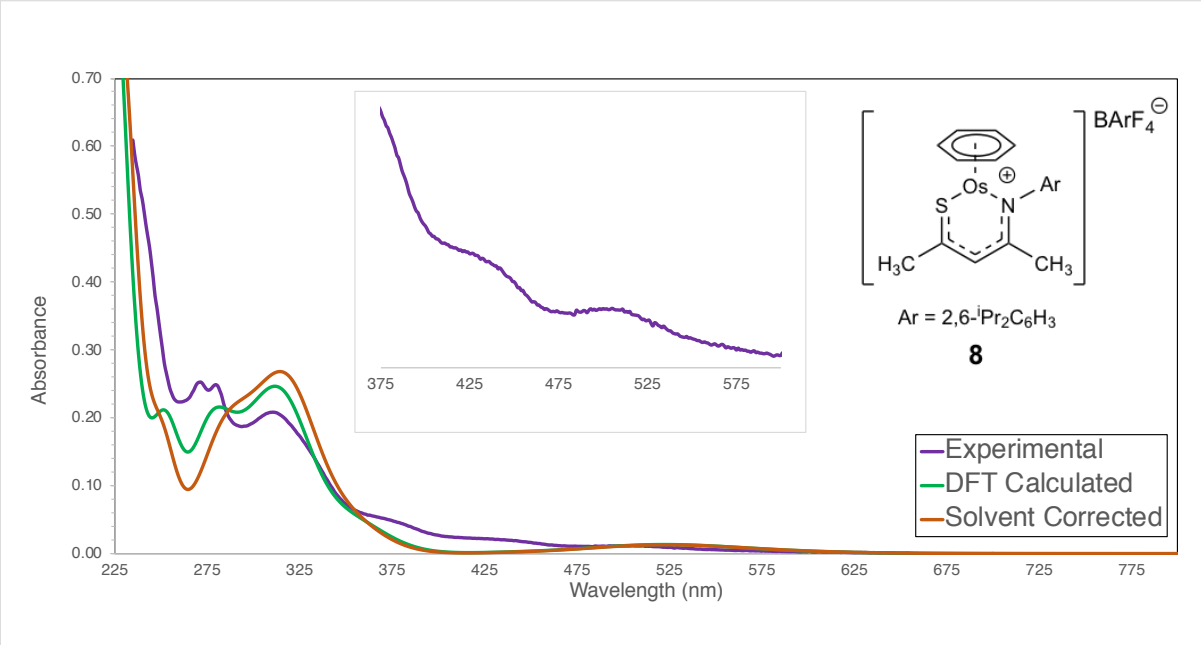

Figure S11: Comparison of experimental (CH_2Cl_2), TD-DFT (ωB97XD, gas phase) and TD-DFT (ωB97XD, CPCM-CH_2Cl_2 corrected) optical absorption spectra for cationic η^6-C_6H_6 Os *N*-2,6-diisopropyl-phenyl-β-thioketoiminate. The inset shows the weak and board experimental absorptions at 507 and 432 nm.

References

1. Rigaku CrysAlis *CCD and CrysAlis RED* version 1.711.36 **2012**, Oxford Diffraction Ltd, Yarton, Oxfordshire, United Kingdom.
2. Bruker-Nonius. *COLLECT: data collection software*, **1999**, Burker AXIS B.V., Delft, Netherlands.
3. Duisenberg, A. J. M.; Kroon-Batenburg, L. M. J.; Schreurs, A. M. M. *J. Appl. Cryst.* **2003**, 36, 220.
4. Bruker. SAINT V6.28 Data Reduction Software. **2001** Bruker AXS, Madison, Wisconsin, USA
5. Duisenberg, A. J. M. *J. Appl. Cryst.* **1992**, *25*, 92.
6. Bruker *XPREP: Reciprocal Space Exploration, version 6.14*. **2003**, Bruker AXS, Madison, Wisconsin, USA.
7. Sheldrick, G. M. *SADABS: Area detector absorption and other corrections, version 2.06*, **2003**, Bruker-AXS, Madison, Wisconsin, USA.
8. Sheldrick, G. M. Acta Cryst. **2015**, C71, 3-8.
9. Spek, A. L. Acta Cryst. **2015**, C71, 9-18.
10. Farrugia, L. J. *J. Appl. Cryst.* **2012**, 45, 849-854.
11. Phillips, A. D.; Laurenczy, G.; Scopelliti, R.; Dyson, P. J., *Organometallics* **2007,** *26*, 1120-1122.
12. Stender, M.; Wright, R. J.; Eichler, B. E.; Prust, J.; Olmstead, M. M.; Roesky, H. W.; Power, P. P., *Dalton Trans.* **2001**, 3465-3469.
13. Frisch, M. J.; Trucks, G. W.; Schlegel, H. B.; Scuseria, G. E.; Robb, M. A.; Cheeseman, J. R.; Scalmani, G.; Barone, V.; Petersson, G. A.; Nakatsuji, H.; Li, X.; Caricato, M.; Marenich, A. V.; Bloino, J.; Janesko, B. G.; Gomperts, R.; Mennucci, B.; Hratchian, H. P.; Ortiz, J. V.; Izmaylov, A. F.; Sonnenberg, J. L.; Williams-Young, D.; Ding, F.; Lipparini, F.; Egidi, F.; Goings, J.; Peng, B.; Petrone, A.; Henderson, T.; Ranasinghe, D.; Zakrzewski, V. G.; Gao, J.; Rega, N.; Zheng, G.; Liang, W.; Hada, M.; Ehara, M.; Toyota, K.; Fukuda, R.; Hasegawa, J.; Ishida, M.; Nakajima, T.; Honda, Y.; Kitao, O.; Nakai, H.; Vreven, T.; Throssell, K.; Montgomery, J. A., Jr.; Peralta, J. E.; Ogliaro, F.; Bearpark, M. J.; Heyd, J. J.; Brothers, E. N.; Kudin, K. N.; Staroverov, V. N.; Keith, T. A.; Kobayashi, R.; Normand, J.; Raghavachari, K.; Rendell, A. P.; Burant, J. C.; Iyengar, S. S.; Tomasi, J.; Cossi, M.; Millam, J. M.; Klene, M.; Adamo, C.; Cammi, R.; Ochterski, J. W.; Martin, R. L.; Morokuma, K.; Farkas, O.; Foresman, J. B.; Fox, D. J. *Gaussian 09, Revision E.01,* Gaussian, Inc., Wallingford CT, 2009.
14. Gorelsky, S. I.; Lever, A. B. P. *J. Organomet. Chem.* **2001,** *635*, 187-196. Gorelsky, S. I. *AOMix: Program for Molecular Orbital Analysis*, 6.90; 2017.
15. Chai, J.-D.; Head-Gordon, M., *J. Chem. Phys.* **2009,** *131*, 174105.
16. Petersson, G. A.; Al-Laham, M. A.. *The Journal of Chemical Physics* **1991,** *94* (9), 6081-6090.
17. Kaupp, M.; Schleyer, P. v. R.; Stoll, H.; Preuss, H. *The Journal of Chemical Physics* **1991,** *94* (2), 1360-1366.
18. Dolg, M.; Stoll, H.; Preuss, H.; Pitzer, R. M.. *The Journal of Physical Chemistry* **1993,** *97* (22), 5852-5859.
19. Marenich, A. V.; Jerome, S. V.; Cramer, C. J.; Truhlar, D. G. *Journal of chemical theory and computation* **2012,** *8* (2), 527-41.

20. GaussView, Version 6, Dennington, Roy; Keith, Todd A.; Millam, John M. Semichem Inc., Shawnee Mission, KS, **2016**.

21. Shao, Y.; Molnar, L. F.; Jung, Y.; Kussmann, J.; Ochsenfeld, C.; Brown, S. T.; Gilbert, A. T. B.; Slipchenko, L. V.; Levchenko, S. V.; O'Neill, D. P.; DiStasio Jr, R. A.; Lochan, R. C.; Wang, T.; Beran, G. J. O.; Besley, N. A.; Herbert, J. M.; Yeh Lin, C.; Van Voorhis, T.; Hung Chien, S.; Sodt, A.; Steele, R. P.; Rassolov, V. A.; Maslen, P. E.; Korambath, P. P.; Adamson, R. D.; Austin, B.; Baker, J.; Byrd, E. F. C.; Dachsel, H.; Doerksen, R. J.; Dreuw, A.; Dunietz, B. D.; Dutoi, A. D.; Furlani, T. R.; Gwaltney, S. R.; Heyden, A.; Hirata, S.; Hsu, C.-P.; Kedziora, G.; Khalliulin, R. Z.; Klunzinger, P.; Lee, A. M.; Lee, M. S.; Liang, W.; Lotan, I.; Nair, N.; Peters, B.; Proynov, E. I.; Pieniazek, P. A.; Min Rhee, Y.; Ritchie, J.; Rosta, E.; David Sherrill, C.; Simmonett, A. C.; Subotnik, J. E.; Lee Woodcock Iii, H.; Zhang, W.; Bell, A. T.; Chakraborty, A. K.; Chipman, D. M.; Keil, F. J.; Warshel, A.; Hehre, W. J.; Schaefer Iii, H. F.; Kong, J.; Krylov, A. I.; Gill, P. M. W.; Head-Gordon, M., Advances in methods and algorithms in a modern quantum chemistry program package. *Physical Chemistry Chemical Physics* **2006,** *8* (27), 3172-3191.